

Undercomplete Blind Subspace Deconvolution

Zoltán Szabó, Barnabás Póczos, and András Lőrincz

Department of Information Systems, Eötvös Loránd University

Pázmány P. sétány 1/C, Budapest H-1117, Hungary

WWW home page: <http://nipg.info>

sszoli@cs.elte.hu, pbarn@cs.elte.hu, lorincz@inf.elte.hu

Abstract

We introduce the blind subspace deconvolution (BSSD) problem, which is the extension of both the blind source deconvolution (BSD) and the independent subspace analysis (ISA) tasks. We examine the case of the undercomplete BSSD (uBSSD). Applying temporal concatenation we reduce this problem to ISA. The associated ‘high dimensional’ ISA problem can be handled by a recent technique called joint f-decorrelation (JFD). Similar decorrelation methods have been used previously for kernel independent component analysis (kernel-ICA). More precisely, the kernel canonical correlation (KCCA) technique is a member of this family, and, as is shown in this paper, the kernel generalized variance (KGV) method can also be seen as a decorrelation method in the feature space. These kernel based algorithms will be adapted to the ISA task. In the numerical examples, we (i) examine how efficiently the emerging higher dimensional ISA tasks can be tackled, and (ii) explore the working and advantages of the derived kernel-ISA methods.

1 Introduction

Independent component analysis (ICA) [1, 2] aims to recover linearly or non-linearly mixed independent and hidden sources. There is a broad range of applications for ICA, such as blind source separation, feature extraction and denoising. Particular applications include the analysis of financial and neurobiological data, fMRI, EEG, and MEG. For recent review concerning ICA the reader is referred to the literature [3, 4].

Traditional ICA algorithms are one-dimensional in the sense that all sources are assumed to be independent real valued random variables. Nonetheless, applications in which only certain groups of sources are independent may be highly relevant in practice. In this case, the independent sources can be multidimensional. For instance, consider the generalization of the cocktail-party problem, where *independent groups of people* are talking about independent topics or more than one *group of musicians* is playing at the party. The separation task requires an extension of ICA, which can be called independent subspace analysis (ISA) [5], multidimensional independent component analysis (MICA) [6], and group ICA [7]. We will use the first of these abbreviations throughout this paper.

Strenuous efforts have been made to develop ISA algorithms [6, 8, 5, 9, 10, 11, 12, 13, 14, 7, 15, 16, 17, 18]. For the most part, ISA-related theoretical problems concern the estimation of entropy or of mutual information. For this, the k -nearest neighbors [13] and the geodesic spanning tree methods [14] can be applied. Other recent approaches seek independent subspaces via kernel methods [11] and joint block diagonalization [7, 16].

Another extension of the original ICA task is the blind source deconvolution (BSD) problem. Such a problem emerges, for example, at a cocktail-party being held in an *echoic room*. Several BSD algorithms were developed in the past. See, for example, the review of [19]. Like ICA, BSD has several applications: (i) remote sensing applications; passive radar/sonar processing [20, 21], (ii) image-deblurring, image restoration [22], (iii) speech enhancement using microphone arrays, acoustics [23, 24, 25, 26], (iv) multi-antenna wireless communications,

sensor networks [27, 28], (v) biomedical signal—EEG, ECG, MEG, fMRI—analysis [29, 30, 31], (vi) optics [32], (vii) seismic exploration [33].

The simultaneous assumption of the two extensions, that is, ISA combined with BSD, seems to be a more realistic model than either of the two models alone. For example, at the cocktail-party, groups of people or groups of musicians may form independent source groups and echoes could be present. This task will be called blind subspace deconvolution (BSSD). We treat the undercomplete case (uBSSD) here. In terms of the cocktail-party problem, it is assumed that there are more microphones than acoustic sources. Here we note that the complete, and in particular the overcomplete, BSSD task is challenging and as of yet no general solution is known. We can show that temporal concatenation turns the uBSSD task into an ISA problem. One of the most stringent applications of BSSD could be the analysis of EEG or fMRI signals. The ICA assumptions could be highly problematic here, because some sources may depend one another, so an ISA model seems better. Furthermore, the passing of information from one area to another and the related delayed and transformed activities may be modeled as echoes. Thus, one can argue that BSSD may fit this important problem domain better than ICA or even ISA.

In principle, the ISA problem can be treated with the methods listed above. However, the dimension of the ISA problem derived from an uBSSD task is not amenable to state-of-the-art ISA methods. According to a recent decomposition principle, the ISA Separation Theorem [34], the ISA task can be divided into two consecutive steps under certain conditions: after the application of the ICA algorithm, the ICA elements need to be grouped.¹ The importance of this direction stems from the fact that ICA methods can deal with problems in high dimensions. The derived ISA task will be solved with the use of the decomposition principle augmented by the joint f-decorrelation (JFD) technique [17].

We show other ISA approaches beyond the JFD method: We adapted the kernel canonical correlation analysis (KCCA) and the kernel generalized variance (KGV) methods [36] to measure the mutual dependency of multidimensional variables. One can show that similarly to the JFD and the KCCA methods, the KGV technique deals with nonlinear decorrelation in function spaces. We found that they can be more precise but are limited to smaller problems.

The paper is structured as follows: Section 2 formulates the problem domain. Section 3 shows how to transform the uBSSD task into an ISA task. The JFD method, which we use to solve the derived ISA task, is the subject of Section 4. This section also addresses how to tailor the KCCA and KGV kernel-ICA methods to solve the ISA problem. Section 5 contains the numerical illustrations and conclusions are drawn in Section 6.

2 The BSSD and the ISA Model

The BSSD task and its special case, the ISA model, are defined in Section 2.1. Section 2.2 details the ambiguities of the ISA task. Section 2.3 introduces some possible ISA cost functions.

2.1 The BSSD Equations

Here, we define the BSSD task. Assume that we have M hidden, independent, multidimensional *components* (random variables). Suppose also that only their casual FIR filtered mixture is available for observation:²

$$\mathbf{x}(t) = \sum_{l=0}^L \mathbf{H}_l \mathbf{s}(t-l), \quad (1)$$

where $\mathbf{s}(t) = [\mathbf{s}^1(t); \dots; \mathbf{s}^M(t)] \in \mathbb{R}^{Md}$ is a vector concatenated of components $\mathbf{s}^m(t) \in \mathbb{R}^d$. For a given m , $\mathbf{s}^m(t)$ is i.i.d. (independent and identically distributed) in time t , \mathbf{s}^m s are non-Gaussian, and $I(\mathbf{s}^1, \dots, \mathbf{s}^M) = 0$, where

¹The possibility of such a decomposition principle was suspected by [6], who based his conjecture on numerical experiments. To the best of our knowledge, a proof encompassing sufficient conditions for this intriguing hypothesis was first published by [35].

²Causal: $l \geq 0$ in \sum_l . FIR: the number of terms in the sum is finite.

I stands for the mutual information of the arguments. The total dimension of the components is $D_s := Md$, the dimension of the observation \mathbf{x} is D_x . Matrices $\mathbf{H}_l \in \mathbb{R}^{D_x \times D_s}$ ($l = 0, \dots, L$) describe the mixing, these are the *mixing matrices*. Without any loss of generality it may be assumed that $E[\mathbf{s}] = \mathbf{0}$, where E denotes the expectation value. Then $E[\mathbf{x}] = \mathbf{0}$ holds, as well. The goal of the BSSD problem is to estimate the original source $\mathbf{s}(t)$ by using observations $\mathbf{x}(t)$ only.

The case $L = 0$ corresponds to the ISA task, and if $d = 1$ also holds then the ICA task is recovered. In the BSD task $d = 1$ and L is a non-negative integer. $D_x > D_s$ is the *undercomplete*, $D_x = D_s$ is the *complete*, and $D_x < D_s$ is the *overcomplete* task. Here, we treat the undercomplete BSSD (uBSSD) problem. We will transform the uBSSD task to undercomplete ISA (uISA) or to complete ISA. From now on they both will be called ISA.

Note 1 *Mixing matrices \mathbf{H}_l ($0 \leq l \leq L$) have a one-to-one mapping to polynomial matrix³ $\mathbf{H}[z] := \sum_{l=0}^L \mathbf{H}_l z^{-l} \in \mathbb{R}[z]^{D_x \times D_s}$, where z is the time-shift operation, that is $(z^{-1}\mathbf{u})(t) = \mathbf{u}(t-1)$. $\mathbf{H}[z]$ may be regarded as an operation that maps D_s -dimensional series to D_x -dimensional series. Equation (1) can be written as $\mathbf{x} = \mathbf{H}[z]\mathbf{s}$.*

Note 2 *It can be shown [37] that in the uBSSD task $\mathbf{H}[z]$ has a polynomial matrix left inverse $\mathbf{W}[z] \in \mathbb{R}[z]^{D_s \times D_x}$ with probability 1, under mild conditions. In other words, for these polynomial matrices $\mathbf{W}[z]$ and $\mathbf{H}[z]$, $\mathbf{W}[z]\mathbf{H}[z]$ is the identity mapping. The mild condition is as follows: Coefficients of polynomial matrix $\mathbf{H}[z]$, that is, random matrix $[\mathbf{H}_0; \dots; \mathbf{H}_L]$ is drawn from a continuous distribution. Under this condition, hidden source $\mathbf{s}(t)$ can be estimated by a suitable causal FIR filtered form of observation $\mathbf{x}(t)$.*

For the uBSSD task it is assumed that $\mathbf{H}[z]$ has a polynomial matrix left inverse. For the uISA and ISA tasks it is supposed that *mixing matrix* $\mathbf{H}_0 \in \mathbb{R}^{D_x \times D_s}$ has full column rank, that is its rank is D_s .

2.2 Ambiguities of the ISA Model

Because the uBSSD task will be reduced to ISA, it is important to see the ambiguities of the ISA task. First, the complete ISA problem ($L = 0, D_x = D_s$) is presented, the undercomplete ISA will be treated later.

The identification of the ISA model is ambiguous. However, the ambiguities are simple [38]: hidden multidimensional components can be determined up to permutation and up to invertible transformation within the subspaces. Ambiguities within the subspaces can be weakened. Namely, because of the invertibility of mixing matrix $\mathbf{H}[z] = \mathbf{H}_0 \in \mathbb{R}^{D_s \times D_s}$, it can be assumed without any loss of generality that both the sources and the observation are *white*, that is,

$$\begin{aligned} E[\mathbf{s}] &= \mathbf{0}, \text{cov}[\mathbf{s}] = \mathbf{I}_{D_s}, \\ E[\mathbf{x}] &= \mathbf{0}, \text{cov}[\mathbf{x}] = \mathbf{I}_{D_x}, \end{aligned}$$

where \mathbf{I}_{D_s} is the D_s -dimensional identity matrix and *cov* is the covariance matrix. It then follows that the mixing matrix \mathbf{H}_0 and thus the *demixing matrix* $\mathbf{W} = \mathbf{H}_0^{-1}$ are orthogonal:

$$\mathbf{I}_{D_s} = \text{cov}[\mathbf{x}] = E[\mathbf{x}\mathbf{x}^*] = \mathbf{H}_0 E[\mathbf{s}\mathbf{s}^*] \mathbf{H}_0^* = \mathbf{H}_0 \mathbf{I}_{D_s} \mathbf{H}_0^* = \mathbf{H}_0 \mathbf{H}_0^*,$$

where $*$ denotes transposition. In sum, $\mathbf{H}_0, \mathbf{W} \in \mathcal{O}^{D_s}$, where \mathcal{O}^{D_s} denotes the set of D_s -dimensional orthogonal matrices. Now, \mathbf{s}^m sources are determined up to permutation and orthogonal transformation.

In order to transform the undercomplete ISA task into a complete ISA task with white observations let $\mathbf{C} := \text{cov}[\mathbf{x}] = E[\mathbf{x}\mathbf{x}^*] = \mathbf{H}_0 \mathbf{H}_0^* \in \mathbb{R}^{D_x \times D_x}$ denote the covariance matrix of the observation. Rank of \mathbf{C} is D_s , since the rank of matrix \mathbf{H}_0 is D_s according to our assumptions. Matrix \mathbf{C} is symmetric ($\mathbf{C} = \mathbf{C}^*$), thus it

³ $\mathbf{H}[z]$ is also known as *channel matrix* or *transfer function* in the literature.

can be decomposed as follows: $\mathbf{C} = \mathbf{U}\mathbf{D}\mathbf{U}^*$, where $\mathbf{U} \in \mathbb{R}^{D_x \times D_s}$, and the columns of matrix \mathbf{U} are orthogonal, that is, $\mathbf{U}^*\mathbf{U} = \mathbf{I}_{D_s}$. Furthermore, the rank of diagonal matrix $\mathbf{D} \in \mathbb{R}^{D_s \times D_s}$ is D_s . The principal component analysis can provide a decomposition in the desired form. Let $\mathbf{Q} := \mathbf{D}^{-1/2}\mathbf{U}^* \in \mathbb{R}^{D_s \times D_x}$. Then the original observation \mathbf{x} can be modified to $\mathbf{x}' := \mathbf{Q}\mathbf{x} = \mathbf{Q}\mathbf{H}_0\mathbf{s} \in \mathbb{R}^{D_s}$. The resulting \mathbf{x}' is white and can be regarded as the observation of a *complete* ISA task having mixing matrix $\mathbf{Q}\mathbf{H}_0 \in \mathcal{O}^{D_s}$.

2.3 ISA Cost Functions

After the whitening procedure (Section 2.2), the ISA task can be viewed as the minimization of the mutual information between the estimated components on the orthogonal group:

$$J_I(\mathbf{W}) := I(\mathbf{y}^1, \dots, \mathbf{y}^M), \quad (2)$$

where $\mathbf{y} = \mathbf{W}\mathbf{x}$, $\mathbf{y} = [\mathbf{y}^1; \dots; \mathbf{y}^M]$, $\mathbf{y}^m \in \mathbb{R}^d$, and $\mathbf{W} \in \mathcal{O}^D$. This formulation of the ISA task serves us in Section 4.1, where we estimate the dependencies of the multidimensional variables.

The ISA task can be rewritten into the minimization of the sum of Shannon's multidimensional differential entropies [13]:

$$J_H(\mathbf{W}) := \sum_{m=1}^M H(\mathbf{y}^m), \quad (3)$$

where $\mathbf{y} = \mathbf{W}\mathbf{x}$, $\mathbf{y} = [\mathbf{y}^1; \dots; \mathbf{y}^M]$, $\mathbf{y}^m \in \mathbb{R}^d$, $\mathbf{W} \in \mathcal{O}^D$.

Note 3 *Until now, we formulated the ISA task by means of the entropy or the mutual information of multidimensional random variables, see Equations (2) and (3). However, any algorithm that treats mutual information between 1-dimensional random variables can also be sufficient. This statement is based on the considerations below. Well-known identities of mutual information and entropy expressions [39] show that the minimization of cost function*

$$J_{H,I}(\mathbf{W}) := \sum_{m=1}^M \sum_{i=1}^d H(y_i^m) - \sum_{m=1}^M I(y_1^m, \dots, y_d^m),$$

or that of

$$J_{I,I}(\mathbf{W}) := I(y_1^1, \dots, y_d^M) - \sum_{m=1}^M I(y_1^m, \dots, y_d^m)$$

can also solve the ISA task. Here, $\mathbf{y} = \mathbf{W}\mathbf{x}$ is the estimated ISA source, where $\mathbf{x} \in \mathbb{R}^D$ is the whitened observation in the ISA model. $\mathbf{W} \in \mathcal{O}^D$ is the estimated ISA demixing matrix, and in $\mathbf{y} = [\mathbf{y}^1; \dots; \mathbf{y}^M] \in \mathbb{R}^D$ the $\mathbf{y}^m \in \mathbb{R}^d$, $m = 1, \dots, M$, represent the estimated components with coordinates $y_i^m \in \mathbb{R}$. The first term of both cost functions $J_{H,I}$ and $J_{I,I}$ is an ICA cost function. Thus, these first terms can be fixed by means of ICA preprocessing.⁴ In this case, if the Separation Theorem holds (for details see Section 3.2), then term $\sum_{m=1}^M I(y_1^m, \dots, y_d^m)$ implies that the maximization of the sum of mutual information between 1-dimensional random variables within the subspaces is sufficient for solving the ISA task.

3 Reduction Steps

Here we show that the direct search for inverse FIR filter can be circumvented (Note 2). Namely, temporal concatenation reduces the uBSSD task to an (u)ISA problem (Section 3.1). Our earlier results will allow further simplifications. We will reduce the ISA task to an ICA task plus a search for optimal permutation of

⁴From the algorithmic point of view, any ICA algorithm that minimizes cost function $I(y_1^1, \dots, y_d^M)$ suits the ICA preprocessing step.

the ICA coordinates. This decomposition principle will be elaborated in Section 3.2 by means of the Separation Theorem.

3.1 Reduction of uBSSD to (u)ISA

We reduce the uBSSD task to an ISA problem. The BSD literature provides the basis for our reduction; [40] use temporal concatenation in their work. This method can be extended to multidimensional \mathbf{s}^m components in a natural fashion:

Let L' be such that

$$D_x L' \geq D_s(L + L') \quad (4)$$

is fulfilled. Such L' exists due to the undercomplete assumption $D_x > D_s$:

$$L' \geq \left\lceil \frac{D_s L}{D_x - D_s} \right\rceil. \quad (5)$$

This choice of L' guarantees that the reduction gives rise to an (under)complete ISA task: let $x_m(t)$ denote the m^{th} coordinate of observation $\mathbf{x}(t)$ and let the matrix $\mathbf{H}_l \in \mathbb{R}^{D_x \times Md}$ be decomposed into $1 \times d$ sized blocks. That is, $\mathbf{H}_l = [\mathbf{H}_l^{ij}]_{i=1..D_x, j=1..M}$ ($\mathbf{H}_l^{ij} \in \mathbb{R}^{1 \times d}$), where i and j denote row and column indices, respectively. Using notations

$$\begin{aligned} \mathbf{S}^m(t) &:= [\mathbf{s}^m(t); \mathbf{s}^m(t-1); \dots; \mathbf{s}^m(t-(L+L')+1)] \in \mathbb{R}^{d(L+L')}, \\ \mathbf{X}^m(t) &:= [x_m(t); x_m(t-1); \dots; x_m(t-L'+1)] \in \mathbb{R}^{L'}, \\ \mathbf{S}(t) &:= [\mathbf{S}^1(t); \dots; \mathbf{S}^M(t)] \in \mathbb{R}^{Md(L+L')=D_s(L+L')}, \\ \mathbf{X}(t) &:= [\mathbf{X}^1(t); \dots; \mathbf{X}^{D_x}(t)] \in \mathbb{R}^{D_x L'}, \\ \mathbf{A}^{ij} &:= \begin{bmatrix} \mathbf{H}_0^{ij} & \dots & \mathbf{H}_L^{ij} & \mathbf{0} & \dots & \mathbf{0} \\ & \ddots & & \ddots & & \\ & & \ddots & & \ddots & \\ \mathbf{0} & \dots & \mathbf{0} & \mathbf{H}_0^{ij} & \dots & \mathbf{H}_L^{ij} \end{bmatrix} \in \mathbb{R}^{L' \times d(L+L')}, \\ \mathbf{A} &:= [\mathbf{A}^{ij}]_{i=1..D_x, j=1..M} \in \mathbb{R}^{D_x L' \times Md(L+L')=D_x L' \times D_s(L+L')}, \end{aligned}$$

model

$$\mathbf{X}(t) = \mathbf{A}\mathbf{S}(t) \quad (6)$$

can be obtained. Here, $\mathbf{s}^m(t)$ s are i.i.d. in time t , they are independent for different m values, and Equation (4) holds for L' . Thus, (6) is either an undercomplete or a complete ISA task, depending on the relation of the l.h.s and the r.h.s of (4): the task is complete if the two sides are equal. The number of the components and the dimension of the components in task (6) are $M(L+L')$ and d , respectively.

If we end up with an undercomplete ISA problem in (6) then it can be reduced to a complete one, as was shown in Section 2.2. Thus, choosing the minimal value for L' in (5), the dimension of the obtained ISA task is

$$D_{\text{ISA}} := D_s(L+L') = D_s \left(L + \left\lceil \frac{D_s L}{D_x - D_s} \right\rceil \right). \quad (7)$$

Taking into account the ambiguities of the ISA task (Section 2.2), the original \mathbf{s}^m components will occur $L+L'$ times and up to orthogonal transformations. As a result, in the ideal case, our estimations are as follows

$$\hat{\mathbf{s}}_k^m := \mathbf{F}_k^m \mathbf{s}^m \in \mathbb{R}^d,$$

where $k = 1, \dots, L+L'$, $\mathbf{F}_k^m \in \mathcal{O}^d$.

3.2 Reduction of ISA to ICA

The Separation Theorem [34] conjectured by [6] allows one to decompose the solution of the ISA problem, under certain conditions, into 2 steps: In the first step, ICA estimation is executed by minimizing $I(y_1^1, \dots, y_d^M)$. In the second step, the ICA elements are grouped by finding an optimal permutation. This principle will be formalized in Section 3.2.1. Section 3.2.2 provides sufficient conditions for the theorem.

3.2.1 The ISA Separation Theorem

We state the ISA Separation Theorem for components having possibly different d_m dimensions:

Theorem 1 (Separation Theorem for ISA) *Let $\mathbf{y} = [y_1; \dots; y_D] = \mathbf{W}\mathbf{x} \in \mathbb{R}^D$, where $\mathbf{W} \in \mathcal{O}^D$, $\mathbf{x} \in \mathbb{R}^D$ is the whitened observation of the ISA model, and $D = \sum_{m=1}^M d_m$. Let \mathcal{S}^{d_m} denote the surface of the d_m -dimensional unit sphere, that is $\mathcal{S}^{d_m} := \{\mathbf{w} \in \mathbb{R}^{d_m} : \sum_{i=1}^{d_m} w_i^2 = 1\}$.*

Presume that the $\mathbf{u} := \mathbf{s}^m \in \mathbb{R}^{d_m}$ sources ($m = 1, \dots, M$) of the ISA model satisfy condition

$$H\left(\sum_{i=1}^{d_m} w_i u_i\right) \geq \sum_{i=1}^{d_m} w_i^2 H(u_i), \forall \mathbf{w} \in \mathcal{S}^{d_m}, \quad (8)$$

and that the ICA cost function $J_{ICA}(\mathbf{W}) = \sum_{i=1}^D H(y_i)$ has minimum over the orthogonal matrices in \mathbf{W}_{ICA} . Then it is sufficient to search for the solution to the ISA task as a permutation of the solution of the ICA task. Using the concept of demixing matrices, it is sufficient to explore forms

$$\mathbf{W}_{ISA} = \mathbf{P}\mathbf{W}_{ICA},$$

where $\mathbf{P} \in \mathbb{R}^{D \times D}$ is a permutation matrix to be determined and \mathbf{W}_{ISA} is the ISA demixing matrix.

The proof of the theorem is presented in Appendix A. It is intriguing that if (8) is satisfied then the simple decomposition principle provides the *global* minimum of (2). In the literature on joint block diagonalization (JBD) [41] have put forth a similar *conjecture* recently. According to this conjecture, for quadratic cost function, if Jacobi optimization is applied, the block-diagonalization of the matrices can be found by the optimization of permutations following the joint diagonalization of the matrices. ISA solutions formulated within the JBD framework [7, 15, 16, 17] make efficient use of this idea in practice. [16] could justify this approach for *local* minimum points.

3.2.2 Sufficient Conditions of the ISA Separation Theorem

The question of which types of sources satisfy the Separation Theorem is open. Equation (8) provides only a sufficient condition. Below, we list sources \mathbf{s}^m that satisfy (8). Details and the extension of the Separation Theorem for complex variables can be found in a technical report of [34].

1. Assume that variables $\mathbf{u} = \mathbf{s}^m$ satisfy the so-called w-EPI condition (EPI is shorthand for the *entropy power inequality* [39]), that is,

$$e^{2H(\sum_{i=1}^d w_i u_i)} \geq \sum_{i=1}^d e^{2H(w_i u_i)}, \forall \mathbf{w} \in \mathcal{S}^d. \quad (9)$$

Then inequality (8) holds for these variables too. The proof can be found in Lemma 1 of Appendix A.

2. The (9) w-EPI condition is valid

- (a) for spherically symmetric or shortly spherical variables [42]. The distribution of such variables is invariant for orthogonal transformations.⁵ Sketch of the proof ($\mathbf{u} = \mathbf{s}^m$): the w-EPI condition concerns projections to unit vectors. For spherical variables, the distribution and thus the entropy of these projections are independent of $\mathbf{w} \in \mathcal{S}^d$. Because $e^{2H(w_i u_i)} = e^{2H(u_i)} w_i^2$ and $\mathbf{w} \in \mathcal{S}^d$, the w-EPI is satisfied with equality $\forall \mathbf{w} \in \mathcal{S}^d$. \square
- (b) for 2-dimensional variables invariant to 90° rotation. Under this condition, density function h of component \mathbf{s}^m is subject to the following invariance

$$h(u_1, u_2) = h(-u_2, u_1) = h(-u_1, -u_2) = h(u_2, -u_1) \quad (\forall \mathbf{u} \in \mathbb{R}^2).$$

Sketch of the proof ($\mathbf{u} = \mathbf{s}^m$): Assume that function $f : \mathcal{S}^2 \ni \mathbf{w} \mapsto H\left(\sum_{i=1}^d w_i u_i\right)$ has global minimum on set $\mathcal{S}^2 \cap \{\mathbf{w} \geq \mathbf{0}\}$.⁶ Let this minimum be at $\mathbf{w}_m \in \mathbb{R}^2$. Then, the 90° invariance warrants that function f take its global minimum also on $\mathbf{w}_m^\perp \in \mathbb{R}^2$, which is perpendicular to \mathbf{w}_m . Let $(\mathbf{C}^m)^* = [\mathbf{w}_m, \mathbf{w}_m^\perp] \in \mathcal{O}^2$. Now, we can estimate variables $\mathbf{C}^m \mathbf{s}^m$. This is sufficient because the ISA solution is ambiguous up to orthogonal transformations within each subspace. \square

A special case of this requirement is invariance to permutation and sign changes

$$h(\pm u_1, \pm u_2) = h(\pm u_2, \pm u_1).$$

In other words, there exists a function $g : \mathbb{R}^2 \rightarrow \mathbb{R}$, which is symmetric in its variables and

$$h(\mathbf{u}) = g(|u_1|, |u_2|).$$

Special cases within this family are distributions

$$h(\mathbf{u}) = g\left(\sum_i |u_i|^p\right) \quad (p > 0),$$

which are constant over the spheres of L^p -space. They are called L^p spherical variables which, for $p = 2$, corresponds to spherical variables.

- (c) for certain weakly dependent variables: [43] has determined sufficient conditions when EPI holds.⁷ If the EPI property is satisfied on unit sphere \mathcal{S}^d , then the ISA Separation Theorem holds (Lemma 1).

These results are summarized schematically in Table 1.

4 ISA Methods

We showed how to convert the uBSSD task to an ISA task in Section 3.1. In the following we will present methods that can solve the ISA task. In Section 4.1 we treat estimations of the mutual information of the ISA cost functions in Section 2.3. Methods that can optimize these cost functions are elaborated in Section 4.2. We also present here the pseudocode of the procedures studied. In Section 4.3 we review methods that can treat non-equal or unknown component dimensions. In what follows, and in accordance with (1), let $\mathbf{x} \in \mathbb{R}^D$ denote the whitened observation, while $\mathbf{y} = [\mathbf{y}^1; \dots; \mathbf{y}^M] = \mathbf{W}\mathbf{x} \in \mathbb{R}^D$ ($\mathbf{W} \in \mathcal{O}^D$) and $\mathbf{y}^m \in \mathbb{R}^d$ ($m = 1, \dots, M$) stand for the estimated source and its components in the ISA task, respectively.

⁵In the ISA task the non-degenerate affine transformations of spherical variables, the so called elliptical variables, do not provide valuable generalizations due to the ambiguities of the ISA task.

⁶Relation $\mathbf{w} \geq \mathbf{0}$ concerns each coordinate.

⁷The constraint of $d = 2$ may be generalized to higher dimensions. We are not aware of such generalizations.

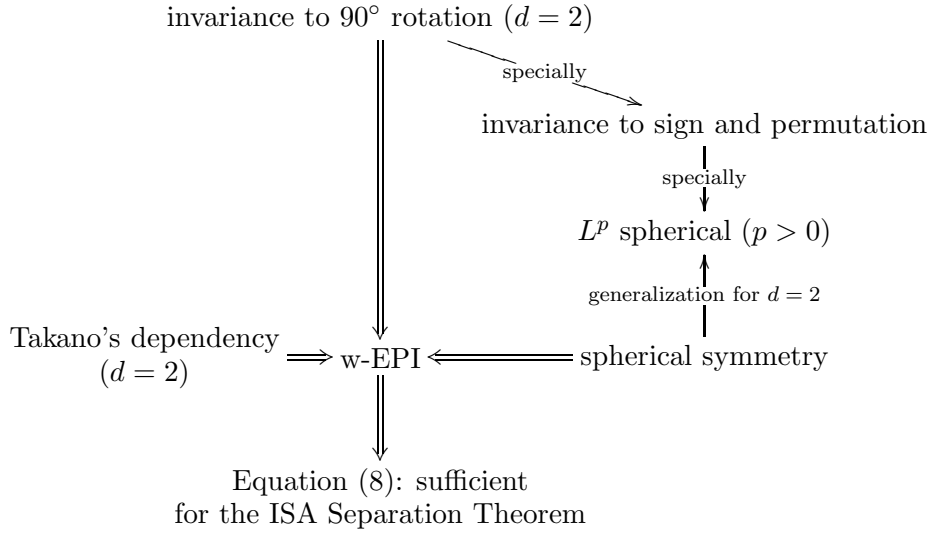


Table 1: Sufficient conditions for the ISA Separation Theorem.

4.1 Dependency Estimations

Here we introduce two dependency estimators. First, in Section 4.1.1 we describe a decorrelation method that uses a set of functions jointly. This method is called joint f-decorrelation (JFD) method [17]. Our second technique (Section 4.1.2) generalizes earlier kernel-ICA methods for the ISA task. The motivation for this latter method is the efficiency and precision of kernel-ICA methods in finding independent components [36]. Our experiences are similar with kernel-ISA methods, see Section 5.3. We found that kernel-ISA methods need more computations, but can provide more precise solutions than the JFD technique.

4.1.1 The JFD Method

The JFD method estimates the hidden \mathbf{s}^m components through the decorrelation over a function set $\mathcal{F}(\ni \mathbf{f})$ [17]. Formally, let the empirical \mathbf{f} -covariance matrix of $\mathbf{y}(t)$ and $\mathbf{y}^m(t)$ for function $\mathbf{f} = [\mathbf{f}^1; \dots; \mathbf{f}^M] \in \mathcal{F}$ over $t = 1, \dots, T$ be denoted by

$$\begin{aligned} \Sigma(\mathbf{f}, T, \mathbf{W}) &= \widehat{\text{cov}}[\mathbf{f}(\mathbf{y}), \mathbf{f}(\mathbf{y})] = \\ &= \frac{1}{T} \sum_{t=1}^T \left\{ \mathbf{f}[\mathbf{y}(t)] - \frac{1}{T} \sum_{k=1}^T \mathbf{f}[\mathbf{y}(k)] \right\} \left\{ \mathbf{f}[\mathbf{y}(t)] - \frac{1}{T} \sum_{k=1}^T \mathbf{f}[\mathbf{y}(k)] \right\}^*, \\ \Sigma^{i,j}(\mathbf{f}, T, \mathbf{W}) &= \widehat{\text{cov}}[\mathbf{f}^i(\mathbf{y}^i), \mathbf{f}^j(\mathbf{y}^j)] = \\ &= \frac{1}{T} \sum_{t=1}^T \left\{ \mathbf{f}^i[\mathbf{y}^i(t)] - \frac{1}{T} \sum_{k=1}^T \mathbf{f}^i[\mathbf{y}^i(k)] \right\} \left\{ \mathbf{f}^j[\mathbf{y}^j(t)] - \frac{1}{T} \sum_{k=1}^T \mathbf{f}^j[\mathbf{y}^j(k)] \right\}^*. \end{aligned}$$

Then, the joint decorrelation on \mathcal{F} can be formulated as the minimization of cost function

$$J_{\text{JFD}}(\mathbf{W}) := \sum_{\mathbf{f} \in \mathcal{F}} \|\mathbf{N} \circ \Sigma(\mathbf{f}, T, \mathbf{W})\|_F^2. \quad (10)$$

Here: (i) $\mathbf{W} \in \mathcal{O}^D$, (ii) \mathcal{F} denotes a set of $\mathbb{R}^D \rightarrow \mathbb{R}^D$ functions, and each function acts on each coordinate separately, (iii) \circ denotes the point-wise multiplication, called the Hadamard-product, (iv) \mathbf{N} masks according

to the subspaces, $\mathbf{N} := \mathbf{E}_D - \mathbf{I}_M \otimes \mathbf{E}_d$, where all elements of matrix $\mathbf{E}_D \in \mathbb{R}^{D \times D}$ and $\mathbf{E}_d \in \mathbb{R}^{d \times d}$ are equal to 1, \otimes is the Kronecker-product, $(\mathbf{v}) \|\cdot\|_F^2$ denotes the square of the Frobenius norm, that is, the sum of the squares of the elements.

Cost function (10) can be interpreted as follows: for *any* function $\mathbf{f}^m : \mathbb{R}^d \rightarrow \mathbb{R}^d$ that acts on independent variables \mathbf{y}^m ($m = 1, \dots, M$) the variables $\mathbf{f}^m(\mathbf{y}^m)$ remain independent. Thus, covariance matrix $\Sigma(\mathbf{f}, T, \mathbf{W})$ of variable $\mathbf{f}(\mathbf{y}) = [\mathbf{f}^1(\mathbf{y}^1); \dots; \mathbf{f}^M(\mathbf{y}^M)]$ is block-diagonal. Independence of estimated sources \mathbf{y}^m is gauged by the uncorrelatedness on the function set \mathcal{F} . Thus, the non-block-diagonal portions $(\Sigma^{i,j}(\mathbf{f}, T, \mathbf{W}), i \neq j)$ of covariance matrices $\Sigma(\mathbf{f}, T, \mathbf{W})$ are punished. This principle is expressed by the term $\|\mathbf{N} \circ \Sigma(\mathbf{f}, T, \mathbf{W})\|_F^2$.

4.1.2 Kernel-ISA Methods

Two alternatives for the ISA cost function of (10) are presented. They estimate the mutual information based ISA cost defined in (2) via kernels: the KCCA and KGV kernel-ICA methods of [36] are extended to the ISA task. The original methods estimate pair-wise independence between *1-dimensional* random variables.⁸ The extension to the multidimensional case is straightforward, the arguments of the kernels can be modified to multidimensional variables and the derivation of [36] can be followed. The main steps are provided below for the sake of completeness. The resulting expressions can be used for the estimation of dependence between multidimensional random variables. The performance of these simple extensions on the related ISA applications is shown in Section 5.3.2.

The KCCA Method First, the 2-variable-case is treated and then it will be generalized to many variables.

2-variable-case Assume that the mutual dependence of two random variables $\mathbf{u} \in \mathbb{R}^{d_1}$ and $\mathbf{v} \in \mathbb{R}^{d_2}$ has to be measured. Let positive semi-definite kernels $k^{\mathbf{u}}(\cdot, \cdot) : \mathbb{R}^{d_1} \times \mathbb{R}^{d_1} \rightarrow \mathbb{R}$, and $k^{\mathbf{v}}(\cdot, \cdot) : \mathbb{R}^{d_2} \times \mathbb{R}^{d_2} \rightarrow \mathbb{R}$ be chosen in the respective spaces. Let $\mathcal{F}^{\mathbf{u}}$ and $\mathcal{F}^{\mathbf{v}}$ denote the reproducing kernel Hilbert spaces (RKHS) [44, 45, 46] associated with the kernels. Here, $\mathcal{F}^{\mathbf{u}}$ and $\mathcal{F}^{\mathbf{v}}$ are function spaces having elements that perform mappings $\mathbb{R}^{d_1} \rightarrow \mathbb{R}$ and $\mathbb{R}^{d_2} \rightarrow \mathbb{R}$, respectively. Then the mutual dependence between \mathbf{u} and \mathbf{v} can be measured, for instance, by the following expression:

$$J_{\text{KCCA}}^*(\mathbf{u}, \mathbf{v}, \mathcal{F}^{\mathbf{u}}, \mathcal{F}^{\mathbf{v}}) := \sup_{g \in \mathcal{F}^{\mathbf{u}}, h \in \mathcal{F}^{\mathbf{v}}} \text{corr}[g(\mathbf{u}), h(\mathbf{v})],$$

where *corr* denotes correlation.

The value of J_{KCCA}^* can be estimated empirically: assume that we have T samples both from \mathbf{u} and from \mathbf{v} . These samples are $\mathbf{u}_1, \dots, \mathbf{u}_T \in \mathbb{R}^{d_1}$ and $\mathbf{v}_1, \dots, \mathbf{v}_T \in \mathbb{R}^{d_2}$. Then, using notations $\bar{g} := \frac{1}{T} \sum_{k=1}^T g(\mathbf{u}_k)$, $\bar{h} := \frac{1}{T} \sum_{k=1}^T g(\mathbf{v}_k)$, the empirical estimation of J_{KCCA}^* could be the following:

$$J_{\text{KCCA}}^{*,\text{emp}}(\mathbf{u}, \mathbf{v}, \mathcal{F}^{\mathbf{u}}, \mathcal{F}^{\mathbf{v}}) := \sup_{g \in \mathcal{F}^{\mathbf{u}}, h \in \mathcal{F}^{\mathbf{v}}} \frac{\frac{1}{T} \sum_{t=1}^T [g(\mathbf{u}_t) - \bar{g}][h(\mathbf{v}_t) - \bar{h}]}{\sqrt{\frac{1}{T} \sum_{t=1}^T [g(\mathbf{u}_t) - \bar{g}]^2} \sqrt{\frac{1}{T} \sum_{t=1}^T [h(\mathbf{v}_t) - \bar{h}]^2}}.$$

However, it is worth including some regularization for J_{KCCA}^* [47], therefore J_{KCCA}^* is modified to

$$J_{\text{KCCA}}(\mathbf{u}, \mathbf{v}, \mathcal{F}^{\mathbf{u}}, \mathcal{F}^{\mathbf{v}}) := \sup_{g \in \mathcal{F}^{\mathbf{u}}, h \in \mathcal{F}^{\mathbf{v}}} \frac{\text{cov}[g(\mathbf{u}), h(\mathbf{v})]}{\sqrt{\text{var}[g(\mathbf{u})] + \kappa \|g\|_{\mathcal{F}^{\mathbf{u}}}^2} \sqrt{\text{var}[h(\mathbf{v})] + \kappa \|h\|_{\mathcal{F}^{\mathbf{v}}}^2}}, \quad (11)$$

⁸We note that if our observations are generated by an ISA model then—unlike in the ICA task when $d = 1$ —pairwise independence is *not* equivalent to mutual independence [2, 14]. Nonetheless, according to our numerical experiences it is an efficient approximation in many situations.

where expression ‘var’ stands for variance, $\kappa > 0$ is the regularization parameter, $\|\cdot\|_{\mathcal{F}^{\mathbf{u}}}^2$ and $\|\cdot\|_{\mathcal{F}^{\mathbf{v}}}^2$ denote the RKHS norm of their arguments in $\mathcal{F}^{\mathbf{u}}$ and $\mathcal{F}^{\mathbf{v}}$, respectively. Now, expanding the denominator up to second order in κ , setting the expectation value of the samples to zero in the respective RKHSs, and using the notation $\kappa_2 := \frac{\kappa T}{2}$ [36], the empirical estimation of (11) is

$$\hat{J}_{\text{KCCA}}^{\text{emp}}(\mathbf{u}, \mathbf{v}, \mathcal{F}^{\mathbf{u}}, \mathcal{F}^{\mathbf{v}}) = \sup_{\mathbf{c}_1 \in \mathbb{R}^T, \mathbf{c}_2 \in \mathbb{R}^T} \frac{\mathbf{c}_1^* \tilde{\mathbf{K}}^{\mathbf{u}} \tilde{\mathbf{K}}^{\mathbf{v}} \mathbf{c}_2}{\sqrt{\mathbf{c}_1^* (\tilde{\mathbf{K}}^{\mathbf{u}} + \kappa_2 \mathbf{I}_T)^2 \mathbf{c}_1} \sqrt{\mathbf{c}_2^* (\tilde{\mathbf{K}}^{\mathbf{v}} + \kappa_2 \mathbf{I}_T)^2 \mathbf{c}_2}}, \quad (12)$$

where $\tilde{\mathbf{K}}^{\mathbf{u}}, \tilde{\mathbf{K}}^{\mathbf{v}} \in \mathbb{R}^{T \times T}$ are the so-called centered kernel matrices: These matrices are derived from kernel matrices $\mathbf{K}^{\mathbf{u}} = [k(\mathbf{u}_i, \mathbf{u}_j)]_{i,j=1,\dots,T}$, $\mathbf{K}^{\mathbf{v}} = [k(\mathbf{v}_i, \mathbf{v}_j)]_{i,j=1,\dots,T} \in \mathbb{R}^{T \times T}$, as is described below. Let $\mathbf{1}_T \in \mathbb{R}^T$ denote a vector whose all elements are equal to 1 and let $\mathbf{H} := \mathbf{I}_T - \frac{1}{T} \mathbf{1}_T \mathbf{1}_T^* \in \mathbb{R}^{T \times T}$ denote the so-called T -dimensional centering matrix. Then $\tilde{\mathbf{K}}^{\mathbf{u}} := \mathbf{H} \mathbf{K}^{\mathbf{u}} \mathbf{H}$, $\tilde{\mathbf{K}}^{\mathbf{v}} := \mathbf{H} \mathbf{K}^{\mathbf{v}} \mathbf{H}$.

Computing the stationary points of $\hat{J}_{\text{KCCA}}^{\text{emp}}$ in (12), that is, setting $\mathbf{0} = \frac{\partial \hat{J}_{\text{KCCA}}^{\text{emp}}}{\partial \mathbf{c}}$, the resulting task is to solve a *generalized eigenvalue problem* of the form $\mathbf{C}\xi = \mu \mathbf{D}\xi$:

$$\begin{pmatrix} (\tilde{\mathbf{K}}^{\mathbf{u}} + \kappa_2 \mathbf{I}_T)^2 & \tilde{\mathbf{K}}^{\mathbf{u}} \tilde{\mathbf{K}}^{\mathbf{v}} \\ \tilde{\mathbf{K}}^{\mathbf{v}} \tilde{\mathbf{K}}^{\mathbf{u}} & (\tilde{\mathbf{K}}^{\mathbf{v}} + \kappa_2 \mathbf{I}_T)^2 \end{pmatrix} \begin{pmatrix} \mathbf{c}_1 \\ \mathbf{c}_2 \end{pmatrix} = (1 + \gamma) \begin{pmatrix} (\tilde{\mathbf{K}}^{\mathbf{u}} + \kappa_2 \mathbf{I}_T)^2 & \mathbf{0} \\ \mathbf{0} & (\tilde{\mathbf{K}}^{\mathbf{v}} + \kappa_2 \mathbf{I}_T)^2 \end{pmatrix} \begin{pmatrix} \mathbf{c}_1 \\ \mathbf{c}_2 \end{pmatrix},$$

where the objective is to maximize $\gamma := \mathbf{c}_1^* \tilde{\mathbf{K}}^{\mathbf{u}} \tilde{\mathbf{K}}^{\mathbf{v}} \mathbf{c}_2$. Our task is to estimate $\hat{J}_{\text{KCCA}}^{\text{emp}}$, the maximum of γ .

Generalization for many variables The KCCA method can be generalized for more than two random variables and can be used to measure pair-wise dependence: Let us introduce the following notations: Let $\mathbf{y}^1 \in \mathbb{R}^{d_1}, \dots, \mathbf{y}^M \in \mathbb{R}^{d_M}$ be random variables. We want to measure the dependence between these variables. Let positive semi-definite kernels $k^m(\cdot, \cdot) : \mathbb{R}^{d_m} \times \mathbb{R}^{d_m} \rightarrow \mathbb{R}$ ($m = 1, \dots, M$) be chosen in the respective spaces. Let \mathcal{F}^m denote the RKHS associated with kernel $k^m(\cdot, \cdot)$. Having T samples $\mathbf{y}_1^m, \dots, \mathbf{y}_T^m$ for all random variables \mathbf{y}^m ($m = 1, \dots, M$), matrices $\mathbf{K}^m := [k^m(\mathbf{y}_i^m, \mathbf{y}_j^m)]_{i,j=1,\dots,T} \in \mathbb{R}^{T \times T}$ and $\tilde{\mathbf{K}}^m := \mathbf{H} \mathbf{K}^m \mathbf{H} \in \mathbb{R}^{T \times T}$ can be created. Let the regularization parameter be chosen as $\kappa > 0$ and let κ_2 denote the auxiliary variable $\kappa_2 := \frac{\kappa T}{2}$. It can be proven that the computation of $\hat{J}_{\text{KCCA}}^{\text{emp}}$ involves the solution of the following generalized eigenvalue problem:

$$\begin{pmatrix} (\tilde{\mathbf{K}}^1 + \kappa_2 \mathbf{I}_T)^2 & \tilde{\mathbf{K}}^1 \tilde{\mathbf{K}}^2 & \dots & \tilde{\mathbf{K}}^1 \tilde{\mathbf{K}}^M \\ \tilde{\mathbf{K}}^2 \tilde{\mathbf{K}}^1 & (\tilde{\mathbf{K}}^2 + \kappa_2 \mathbf{I}_T)^2 & \dots & \tilde{\mathbf{K}}^2 \tilde{\mathbf{K}}^M \\ \vdots & \vdots & \ddots & \vdots \\ \tilde{\mathbf{K}}^M \tilde{\mathbf{K}}^1 & \tilde{\mathbf{K}}^M \tilde{\mathbf{K}}^2 & \dots & (\tilde{\mathbf{K}}^M + \kappa_2 \mathbf{I}_T)^2 \end{pmatrix} \begin{pmatrix} \mathbf{c}_1 \\ \mathbf{c}_2 \\ \vdots \\ \mathbf{c}_M \end{pmatrix} = \lambda \begin{pmatrix} (\tilde{\mathbf{K}}^1 + \kappa_2 \mathbf{I}_T)^2 & \mathbf{0} & \dots & \mathbf{0} \\ \mathbf{0} & (\tilde{\mathbf{K}}^2 + \kappa_2 \mathbf{I}_T)^2 & \dots & \mathbf{0} \\ \vdots & \vdots & \ddots & \vdots \\ \mathbf{0} & \mathbf{0} & \dots & (\tilde{\mathbf{K}}^M + \kappa_2 \mathbf{I}_T)^2 \end{pmatrix} \begin{pmatrix} \mathbf{c}_1 \\ \mathbf{c}_2 \\ \vdots \\ \mathbf{c}_M \end{pmatrix}. \quad (13)$$

Analogously to the two-variable-case, the largest eigenvalue of this task is a measure of the value of the pair-wise dependence of the random variables.

The KGV Method Equation (2) in Section 2.3 indicates that the ISA task can be seen as the minimization of the mutual information. The basic idea of the KGV technique is that—even for non-Gaussian variables—it estimates the mutual information by the Gaussian approximation [36]. Namely, let $\mathbf{y} = [\mathbf{y}^1; \dots, \mathbf{y}^M]$ be

multidimensional normal random variable with covariance matrix \mathbf{C} . Let $\mathbf{C}^{i,j} \in \mathbb{R}^{d_m \times d_m}$ denote the cross-covariance between components of $\mathbf{y}^m \in \mathbb{R}^{d_m}$. The mutual information between components $\mathbf{y}^1, \dots, \mathbf{y}^M$ is [39]:

$$I(\mathbf{y}^1, \dots, \mathbf{y}^M) = -\frac{1}{2} \log \left(\frac{\det \mathbf{C}}{\prod_{m=1}^M \det \mathbf{C}^{m,m}} \right).$$

The quotient $\frac{\det \mathbf{C}}{\prod_{m=1}^M \det \mathbf{C}^{m,m}}$ is called the *generalized variance*. If \mathbf{y} is *not normal*—this is the typical situation in the ISA task—then let us transform the individual components \mathbf{y}^m using feature mapping φ associated with the reproducing kernel and assume that the image is a normal variable. Thus, the cost function

$$J_{\text{KGV}}(\mathbf{W}) := -\frac{1}{2} \log \left[\frac{\det(\mathcal{K})}{\prod_{m=1}^M \det(\mathcal{K}^{m,m})} \right] \quad (14)$$

is associated with the ISA task. In Equation (14) $\phi(\mathbf{y}) := [\varphi(\mathbf{y}^1); \dots; \varphi(\mathbf{y}^M)]$, $\mathcal{K} := \text{cov}[\phi(\mathbf{y})]$, and the sub-matrices are $\mathcal{K}^{i,j} = \text{cov}[\varphi(\mathbf{y}^i), \varphi(\mathbf{y}^j)]$. Expression $\frac{\det(\mathcal{K})}{\prod_{m=1}^M \det(\mathcal{K}^{m,m})}$ is called the *kernel generalized variance* (KGV).

The next theorem shows that the KGV technique can be interpreted as a decorrelation based method:

Theorem 2 *Let $\Sigma \in \mathbb{R}^{D \times D}$ be a positive semi-definite matrix, let $\Sigma^{m,m} \in \mathbb{R}^{d_m \times d_m}$ denote the m^{th} block in the diagonal of matrix Σ , and let $D = \sum_{m=1}^M d_m$. Then the function*

$$0 \leq Q(\Sigma) := -\frac{1}{2} \log \left[\frac{\det(\Sigma)}{\prod_{m=1}^M \det(\Sigma^{m,m})} \right]$$

is 0 iff $\Sigma = \text{blockdiag}(\Sigma^{1,1}, \dots, \Sigma^{M,M})$.

This theorem can be proven for $d_m \geq 1$, as in the case of $d_m = 1$ [39], see the work of [17]. The theorem implies the following:

Corollary *Setting $\Sigma := \mathcal{K}$, the KGV technique is a decorrelation technique according to feature mapping φ . The KGV technique aims at minimizing of cross-covariances $\mathcal{K}^{i,j} = \text{cov}[\varphi(\mathbf{y}^i), \varphi(\mathbf{y}^j)]$ to $\mathbf{0}$.*

We note that the kernel covariance (KC) ICA method [48]—similarly to the KCCA method—can be extended to measure the mutual dependence of multidimensional random variables and thus to solve the ISA task. Again, the computation of the cost function can be converted to the solution of a generalized eigenvalue problem. This eigenvalue problem is provided in Appendix B for the sake of completeness.

Note 4 *The KCCA, KGV and KC methods can estimate only pair-wise dependence. Nonetheless, the joint mutual information can be estimated by recursive methods computing pair-wise mutual information: for the mutual information of random variables $\mathbf{y}^m \in \mathbb{R}^{d_m}$ ($m = 1, \dots, M$) it can be shown that the recursive relation*

$$I(\mathbf{y}^1, \dots, \mathbf{y}^M) = \sum_{m=1}^M I(\mathbf{y}^m, [\mathbf{y}^{m+1}, \dots, \mathbf{y}^M]) \quad (15)$$

holds [39]. Thus, for example, the KCCA eigenvalue problem of (13) can be replaced by pair-wise estimation of mutual information. We note that the tree-dependent component analysis model [11] estimates the joint mutual information from the pair-wise mutual information.

<p>Input of the algorithm ISA observation: $\{\mathbf{x}(t)\}_{t=1,\dots,T}$</p> <p>Optimization⁹ ICA: on the whitened observation $\mathbf{x} \Rightarrow \hat{\mathbf{s}}_{\text{ICA}}$ estimation</p> <p>Permutation search $\mathbf{P} := \mathbf{I}_D$ repeat sequentially for $\forall p \in \mathcal{G}^{m_1}, q \in \mathcal{G}^{m_2} (m_1 \neq m_2)$: if $J(\mathbf{P}_{pq}\mathbf{P}) < J(\mathbf{P})$ $\mathbf{P} := \mathbf{P}_{pq}\mathbf{P}$ end until $J(\cdot)$ decreases in the <i>sweep</i> above</p> <p>Estimation $\hat{\mathbf{s}}_{\text{ISA}} = \mathbf{P}\hat{\mathbf{s}}_{\text{ICA}}$</p>

Table 2: Pseudocode of the ISA Algorithm. Cost J stands for the ISA cost function of JFD, KCCA, or KGV methods. The permutation matrix of the ISA Separation Theorem is the variable of J .

4.2 Optimization of ISA Costs

There are several possibilities to optimize ISA cost functions:

1. Without ICA preprocessing, optimization problems concern either the *Stiefel manifold* [49, 50, 51, 52] or the *flag manifold* [53]. According to our experiences, these gradient based optimization methods may be stuck in poor local minima.
2. According to the ISA Separation Theorem, it may be sufficient to search for optimal permutation of the ICA components provided by ICA preprocessing. We applied greedy permutation search: two coordinates of different subspaces are exchanged provided that this change decreases cost function J . Here, J denotes, for example, J_{JFD} , J_{KCCA} , or J_{KGV} depending on the ISA technique applied. The variable of J is the permutation matrix \mathbf{P} using the parametrization $\mathbf{W}_{\text{ISA}} = \mathbf{P}\mathbf{W}_{\text{ICA}}$. Pseudocode is provided in Table 2. Our experiences show that greedy permutation search is often sufficient for the estimation of the ISA subspaces. However, it is easy to generate examples in which this is not true [14]. In such cases, global permutation search method of higher computational burden may become necessary [35].

4.3 Different and Unknown Component Dimensions

Here we give a quick overview how one can handle situations when the dimensions of the subspaces are unequal, unknown, or both. Note that the introduced uBSSD-ISA reduction, the ISA ambiguities [16] and the Separation Theorem remain the same for subspaces of different dimensions, and thus it is sufficient to consider the ISA problem.

1. If the dimensions of the subspaces are different but known, the ISA task can be solved
 - (a) the mask \mathbf{N} of the JFD method should be modified (see Equation 10).
 - (b) the kernel-ISA methods include this situation; they were introduced for different subspace dimensions.

⁹Let $\mathcal{G}^1, \dots, \mathcal{G}^M$ denote the indices of the $1^{\text{st}}, \dots, M^{\text{th}}$ subspaces, that is, $\mathcal{G}^m := \{(m-1)d+1, \dots, md\}$, and permutation matrix \mathbf{P}_{pq} exchanges coordinates p and q .

2. If the dimension of the hidden source \mathbf{s} is known, but the individual dimensions of components \mathbf{s}^m are not, then clustering can exploit the dependencies between the coordinates of the estimated sources. For example:
 - (a) If we assume that the hidden \mathbf{s} source has block diagonal AR dynamics of the form $\mathbf{s}(t+1) = \mathbf{F}\mathbf{s}(t) + \mathbf{e}(t)$ — $\mathbf{F} = \text{blockdiag}(\mathbf{F}^1, \dots, \mathbf{F}^M)$ —then connectivity of the estimated matrix $\hat{\mathbf{F}}$ may help [54]. One may assume that the i and the j coordinates are ‘ $\hat{\mathbf{F}}$ -connected’ if value $\max\{|\hat{F}_{ij}|, |\hat{F}_{ji}|\}$ is above a certain threshold.
 - (b) Similar considerations can be applied in the ISA problem, for example, by using cumulant based matrices [16].
 - (c) Weaknesses of the threshold based method include (i) the uncertainty in choosing the threshold, and (ii) the fact that the methods are sensitive to the threshold. More robust solutions can be designed if the dependencies, for example, the mutual information amongst the coordinates, are used to construct an adjacency matrix and apply a clustering method for this matrix. One might use, for example, hierarchical [12] or tree-structured clustering methods [11].

5 Illustrations

The efficiency of the algorithms of Section 4 are illustrated. Test cases are introduced in Section 5.1. The quality of the solutions will be measured by the normalized Amari-error, the Amari-index (Section 5.2). Numerical results are presented in Section 5.3.

5.1 Databases

We define five databases to study our identification algorithms. We do not know whether they satisfy (8) or not. According to our experiences, the ISA Separation Theorem works on these examples.

5.1.1 The 3D-geom, the Celebrities and the ABC Database

The first 3 databases are illustrated in Figure 1. In the *3D-geom* test \mathbf{s}^m s were random variables uniformly distributed on 3-dimensional geometric forms ($d = 3$). We chose 6 different components ($M = 6$) and, as a result, the dimension of the hidden source \mathbf{s} is $D_s = 18$. The *celebrities* test has 2-dimensional source components generated from cartoons of celebrities ($d = 2$).¹⁰ Sources \mathbf{s}^m were generated by sampling 2-dimensional coordinates proportional to the corresponding pixel intensities. In other words, 2-dimensional images of celebrities were considered as density functions. $M = 10$ was chosen. In the *ABC* database, hidden sources \mathbf{s}^m were uniform distributions defined by 2-dimensional images ($d = 2$) of the English alphabet. The number of components varied as $M = 2, 5, 10, 15$, and thus the dimension of the source D_s was 4, 10, 20, 30, respectively.

5.1.2 The all-k-independent Database

The d -dimensional hidden components $\mathbf{u} := \mathbf{s}^m$ were created as follows: coordinates $u_i(t)$ ($i = 1, \dots, k$) were uniform random variables on the set $\{0, \dots, k-1\}$, whereas u_{k+1} was set to $\text{mod}(u_1 + \dots + u_k, k)$. In this construction, every k -element subset of $\{u_1, \dots, u_{k+1}\}$ is made of independent variables. This database is called the *all-k-independent* problem [14, 35]. In our simulations $d = k + 1$ was set to 3 or 4 and we used 2 components ($M = 2$). Thus, source dimension D_s was either 6 or 8.

¹⁰See <http://www.smileyworld.com>.

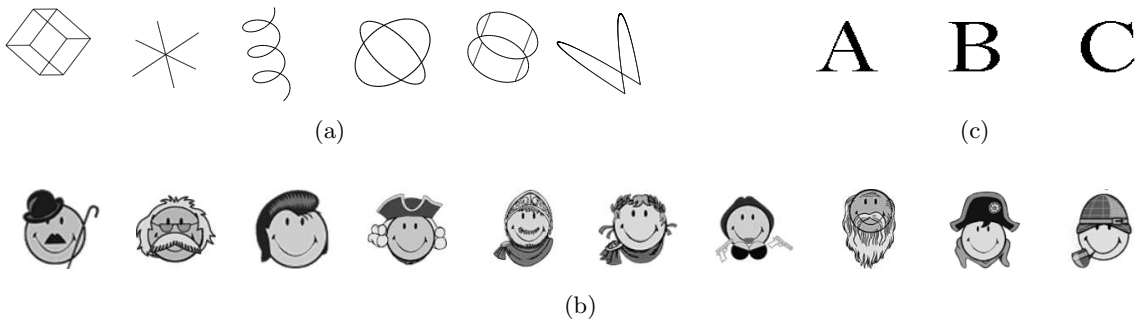


Figure 1: Illustration of the *3D-geom*, *celebrities* and *ABC* databases. (a): database *3D-geom*, 6 3-dimensional components ($M = 6$, $d = 3$). Hidden sources are uniformly distributed variables on 3-dimensional geometric objects. (b): database *celebrities*. Density functions of the hidden sources are proportional to the pixel intensities of the 2-dimensional images ($d = 2$). Number of hidden components: $M = 10$. (c): database *ABC*. Here, the hidden sources \mathbf{s}^m are uniformly distributed on images ($d = 2$) of letters. Number of components M varies between 2 (A and B) and 15 (A-O).

5.1.3 The Beatles Database

Our *Beatles* test is a non-i.i.d. example. Here, hidden sources are stereo Beatles songs.¹¹ 8 kHz sampled portions of two songs (A Hard Day’s Night, Can’t Buy Me Love) made the hidden \mathbf{s}^m s. Thus, the dimension of the components d was 2, the number of the components M was 2, and the dimension of the problem D_s was 4.

5.2 Normalized Amari-error, the Amari-index

We have shown in Section 3.1 that the uBSSD task can be reduced to an ISA task. Consequently, we use ISA performance measure to evaluate our algorithms. Assume that there are M pieces of d -dimensional hidden components in the ISA task, \mathbf{A} is the mixing matrix, and \mathbf{W} is the estimated demixing matrix. Then optimal estimation provides matrix $\mathbf{G} := \mathbf{W}\mathbf{A}$, a block-permutation matrix made of $d \times d$ sized blocks. Let matrix $\mathbf{G} \in \mathbb{R}^{D \times D}$ be decomposed into $d \times d$ blocks: $\mathbf{G} = [\mathbf{G}^{ij}]_{i,j=1,\dots,M}$. Let $g^{i,j}$ denote the sum of the absolute values of the elements of matrix $\mathbf{G}^{i,j} \in \mathbb{R}^{d \times d}$. We used the normalized version [35] of the Amari-error [55] adapted to the ISA task [7, 15] defined as:

$$r(\mathbf{G}) := \frac{1}{2M(M-1)} \left[\sum_{i=1}^M \left(\frac{\sum_{j=1}^M g^{ij}}{\max_j g^{ij}} - 1 \right) + \sum_{j=1}^M \left(\frac{\sum_{i=1}^M g^{ij}}{\max_i g^{ij}} - 1 \right) \right].$$

We refer to the normalized Amari-error as the Amari-index. One can see that $0 \leq r(\mathbf{G}) \leq 1$ for any matrix \mathbf{G} , and $r(\mathbf{G}) = 0$ if and only if \mathbf{G} is a block-permutation matrix with $d \times d$ sized blocks. Normalization is advantageous; we can compare the precision of ISA procedures and procedures, which are reduced to ISA tasks.

5.3 Simulations

Results on databases *3D-geom*, *celebrities*, *ABC*, *all-k-independent* and *Beatles* are provided here. These experimental studies have two main parts:

¹¹See <http://rock.mididb.com/beatles/>.

	$L = 1$	$L = 2$	$L = 3$	$L = 4$	$L = 5$
3D-geom	0.25% (± 0.01)	0.27% (± 0.03)	0.28% (± 0.02)	0.29% (± 0.03)	0.29% (± 0.01)
celebrities	0.37% (± 0.01)	0.38% (± 0.01)	0.39% (± 0.01)	0.39% (± 0.01)	0.40% (± 0.01)

Table 3: The Amari-index of the JFD method for database *3D-geom* and *celebrities*, for different convolution lengths: average \pm deviation. Number of samples: $T = 100,000$. For other sample numbers between $1,000 \leq T < 100,000$ see Figure 2.

1. The efficiency of the JFD method on the uBSSD task is demonstrated in Section 5.3.1.
2. The derived KCCA, KGV kernel-ISA methods were tested on ISA tasks. We show examples in which these methods are favorable over the JFD method in Section 5.3.2.

In both cases the tasks are either ISA tasks or can be reduced to ISA (Section 3.1). Thus, we used the Amari-index (Section 5.2) to measure and compare the performance of the different methods. For each individual parameter, 50 random runs were averaged. Our parameters are: T , the sample number of observations $\mathbf{x}(t)$, L , the parameter of the length of the convolution (the length of the convolution is $L + 1$), M , the number of the components, and d , the dimension of the components, depending on the test. Random run means random choice of quantities $\mathbf{H}[z]$ and \mathbf{s} .

5.3.1 JFD on uBSSD

Our results concerning the uBSSD task are delineated. As we showed in Section 3.1, the temporal concatenation can turn the uBSSD task into an ISA problem. These ISA tasks associated with simple uBSSD problems can easily become more than 100-dimensional. Earlier ISA methods cannot deal with such ‘high dimensional’ problems. This is why we resorted to the recent JFD method (Section 4.1.1), which seemed to be efficient in solving such large problems under the following circumstances: Equation (7) implies that the dimension D_{ISA} of the derived ISA task with fixed L and D_s decreases provided that the difference $D_x - D_s \geq 1$ increases. This coincides with our experiences: the higher this difference is, the smaller number of samples can reach the same precision. Below, studies for $D_x - D_s = D_s$ ($D_x = 2D_s$) are presented. This choice was amenable to the JFD method.¹² In this case the dimension of the ISA task in (7) simplifies to the form

$$D_{\text{ISA}} = 2D_s L.$$

The JFD technique works with the pseudocode given in Table 2: it reduces the uBSSD task to the ISA task, where the fastICA algorithm [56] was chosen to perform the ICA computation. In the JFD cost, we chose manifold \mathcal{F} as $\mathcal{F} := \{\mathbf{u} \rightarrow \cos(\mathbf{u}), \mathbf{u} \rightarrow \cos(2\mathbf{u})\}$, where the functions operated on the coordinates separately [17]. For the ‘observations’, the elements of mixing matrices \mathbf{H}_l in Equation (1) were generated independently from standard normal distributions.¹³

We studied the dependence of the precision versus the sample number on databases *3D-geom* and *celebrities*. The dimension and the number of the components were $d = 3$ and $M = 6$ for the *3D-geom* database and $d = 2$ and $M = 10$ for the *celebrities* database, respectively. In both cases the sample number T varied between 1,000 and 100,000. The parameter of the length of the convolution took $L = 1, \dots, 5$ values. Thus, the length of the convolution changed between 2 and 6. Our results are summarized in Figure 2. The values of the errors are given in Table 3. The number of sweeps needed to optimize the permutations after performing ICA is provided in Figure 3. Figures 4 and 5 illustrate the estimations of the JFD technique on the *3D-geom* and the *celebrities* databases, respectively.

¹²We note that the hardest $D_x - D_s = 1$ task is also feasible. However, the sample number necessary to find the solution grows considerably, as can be expected from (5).

¹³Uniform distribution on $[0,1]$, instead of normal distribution, showed similar performance.

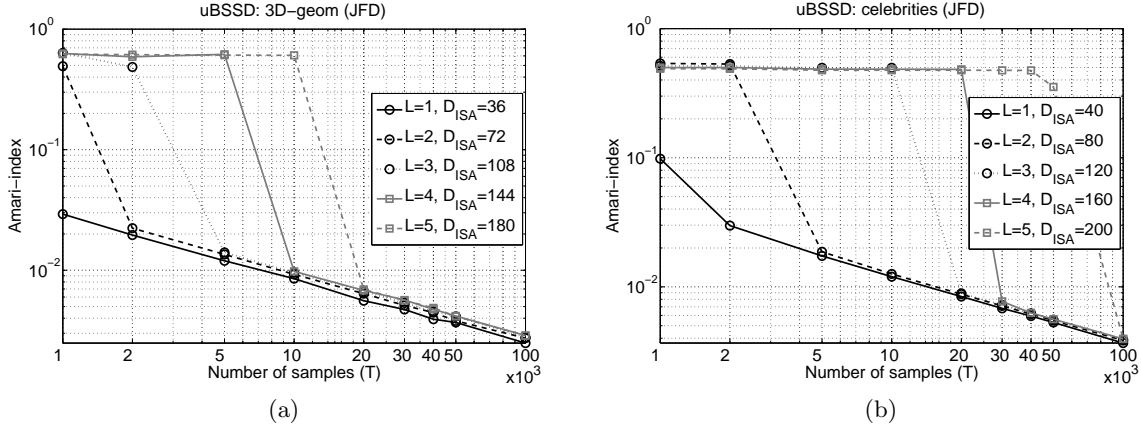


Figure 2: Estimation error of the JFD method on the *3D-geom* and *celebrities* databases: Amari-index as a function of sample number on log-log scale for different convolution lengths. (a): *3D-geom*, (b): *celebrities* database. Dimension of the ISA task: D_{ISA} . For further information, see Table 3.

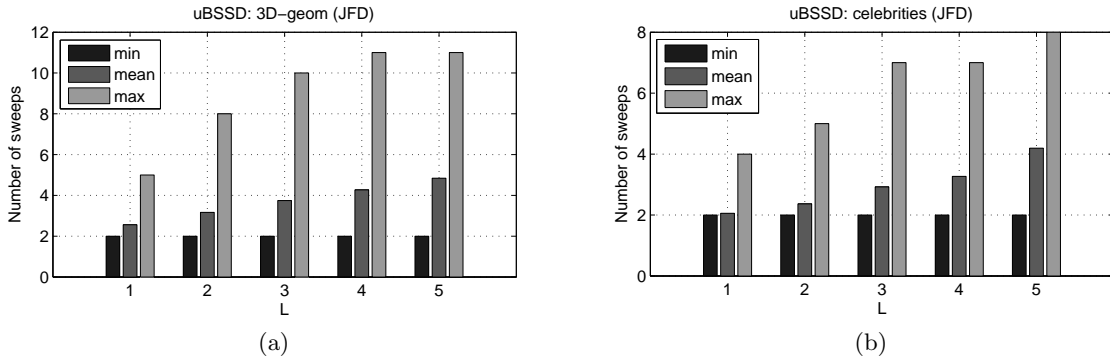


Figure 3: Number of sweeps in permutation search needed for the JFD method as a function of the convolution length. (a): *3D-geom*, (b): *celebrities* database. Black: minimum, gray: average, light gray: maximum.

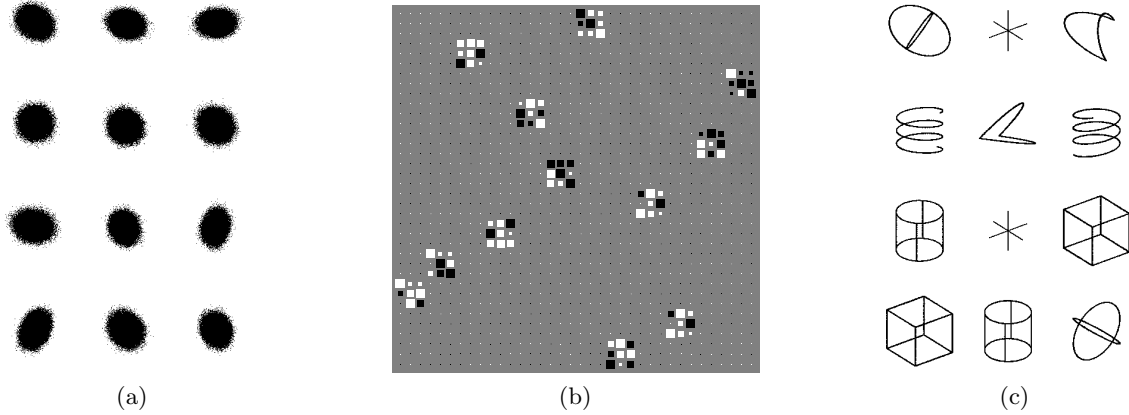


Figure 4: Illustration of the JFD method on the uBSSD task for the *3D-geom* database. Sample number $T = 100,000$, convolution length $L = 1$, Amari-index: 0.25%. (a): observed convolved signals $\mathbf{x}(t)$. (b) Hinton-diagram: the product of the mixing matrix of the derived ISA task and the estimated demixing matrix (= approximately block-permutation matrix with 3×3 blocks). (c): estimated components. Note: hidden components are recovered $L + L' = 2$ times, up to permutation and orthogonal transformation.

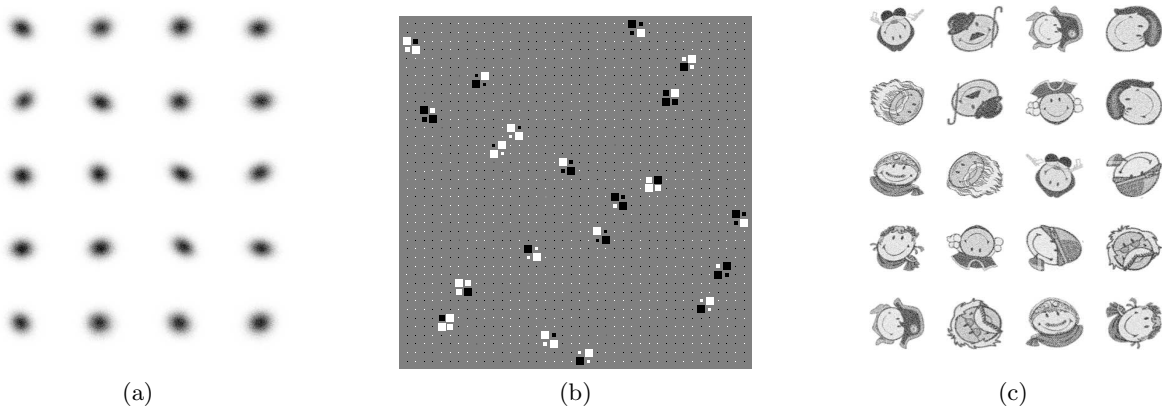


Figure 5: Illustration of the JFD method on the uBSSD task for the *celebrities* database. Sample number $T = 100,000$, convolution length $L = 1$, Amari-index: 0.37%. (a): observed convolved signals $\mathbf{x}(t)$. (b) Hinton-diagram: the product of the mixing matrix of the derived ISA task and the estimated demixing matrix (= approximately block-permutation matrix with 2×2 blocks). (c): estimated components. Note: hidden components are recovered $L + L' = 2$ times, up to permutation and orthogonal transformation.

$L = 1$	$L = 2$	$L = 5$	$L = 10$	$L = 20$	$L = 30$
0.41% (± 0.06)	0.44% (± 0.05)	0.46% (± 0.05)	0.47% (± 0.03)	0.66% (± 0.13)	0.70% (± 0.11)

Table 4: Amari-index of the JFD method for *ABC* database for different convolution lengths: average \pm deviation. Number of samples: $T = 75,000$. For other sample numbers between $1,000 \leq T < 75,000$ see Figure 6(a).

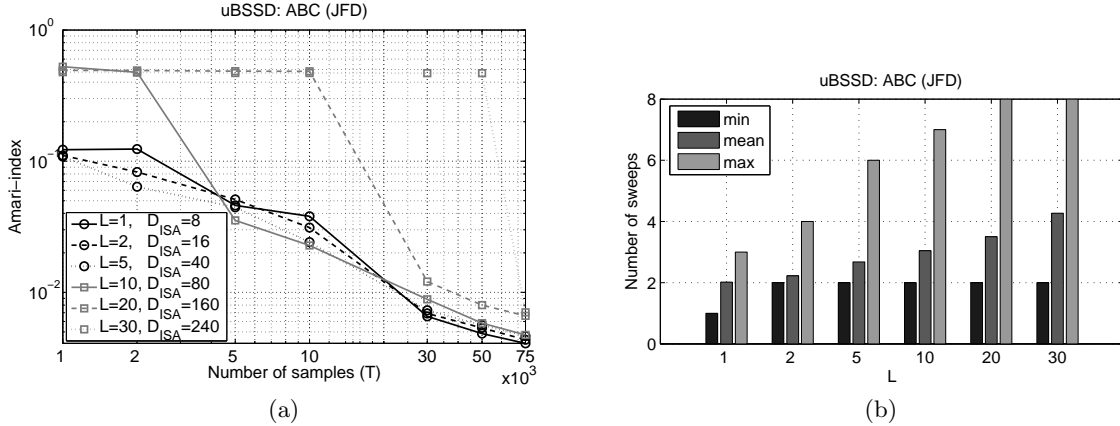


Figure 6: (a): Amari-index of the JFD method on the *ABC* database as a function of sample number and for different convolution lengths on log-log scale. (b): Number of sweeps of permutation optimization on the derived ISA task as a function of convolution length. Dimension of the ISA task: D_{ISA} . Black: minimum, gray: average, light gray: maximum. For further information, see Table 4.

Figure 2 demonstrates that the JFD algorithm was able to uncover the hidden components with high precision. The precision of the estimations shows similar characteristics on the *3D-geom* and the *celebrities* databases. The Amari-index is approximately constant for small sample numbers. For each curve, above a certain threshold the Amari-index decreases suddenly and after the sudden decrease the precision follows a power law $r(T) \propto T^{-c}$ ($c > 0$). The power law decline is manifested by straight line on log-log scale. The slopes of these straight lines are very close to one another. The number of sweeps was between 2 and 11 (2 and 8) for the *3D-geom* (*celebrities*) tests over all sample numbers, for $1 \leq L \leq 5$ and for 50 random initializations. According to Table 3, the Amari-index for sample number $T = 100,000$ is below 1% (0.25 – 0.40%) with small standard deviations (0.01 – 0.03).

In another test the *ABC* database was used. The number and the dimensions of the components were minimal ($d = 2$, $M = 2$) and the dependence on the convolution length was tested. Parameter L took values on 1, 2, 5, 10, 20, 30. The number of observations varied between $1,000 \leq T \leq 75,000$. The Amari-index and the sweep number of the optimization are illustrated in Figure 6. Precise values of the Amari-index are provided in Table 4.

According to Figure 6, the JFD method found the hidden components. The ‘power law’ decline of the Amari-index, which was apparent in the *3D-geom* and the *celebrities* databases, appears for the *ABC* test, too. The figure indicates that for 75,000 samples and for $L = 30$ (convolution length is 31) the problem is still amenable to the JFD technique. The number of sweeps required for the optimization of the permutations was between 1 and 8 for all sample numbers $1,000 \leq T \leq 75,000$, parameters $1 \leq L \leq 30$ and for all 50 random initializations. According to Table 4, for sample number $T = 75,000$ the Amari-index stays below 1% on average (0.41 – 0.7%) and has a small (0.03 – 0.11) standard deviation.

In the case of *Beatles* database, test parameters were similar to those of the *ABC* database: the number and the dimensions of the components were minimal ($d = 2$, $M = 2$) and the dependence on the convolution

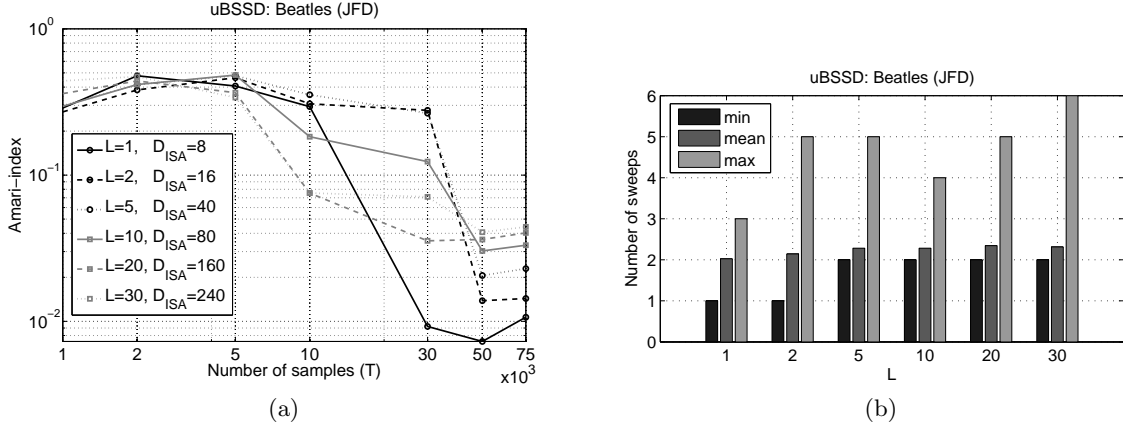


Figure 7: (a): Amari-index of the JFD method on the *Beatles* database as a function of sample number and for different convolution lengths on log-log scale. (b): Number of sweeps of permutation optimization on the derived ISA task as a function of convolution length. Dimension of the ISA task: D_{ISA} . Black: minimum, gray: average, light gray: maximum. For further information, see Table 5.

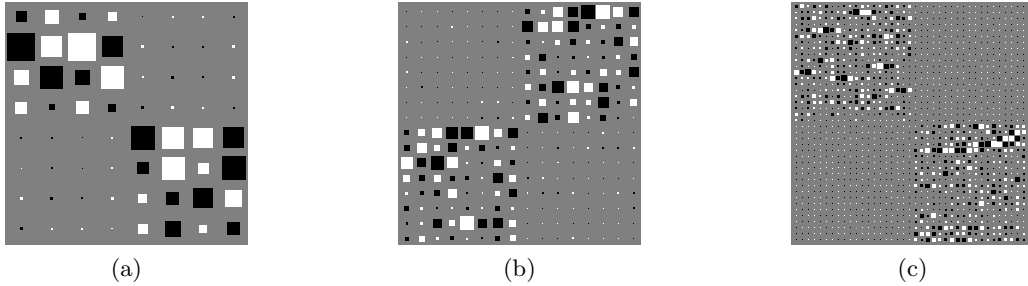


Figure 8: Hinton-diagrams of the JFD methods on the *Beatles* database for different convolution parameters. (a): $L = 1$ ($D_{ISA} = 8$), (b): $L = 2$ ($D_{ISA} = 16$), (c): $L = 5$ ($D_{ISA} = 40$). In the ideal case, 2 pieces of $D_{ISA}/2$ -dimensional blocks are formed by multiplying the mixing matrix of the derived ISA task and the estimated demixing matrix.

length was tested. Parameter L took values on 1, 2, 5, 10, 20, 30. The number of observations varied between $1,000 \leq T \leq 75,000$. The Amari-index and the sweep number of the optimization are illustrated in Figure 7. Precise values of the Amari-index are provided in Table 5. The Hinton-diagrams are in Figure 8.

The *Beatles* songs are non-i.i.d sources and subsequent samples $\mathbf{s}^m(t)$ and $\mathbf{s}^m(t-1)$ have dependencies. Thus, in $\mathbf{S}(t)$ the components of the (6) model that belong to the same song can not be distinguished. In the ideal case, however, the songs can be separated, that is, the separation of the 2 pieces of $(D_{ISA}/2)$ -dimensional song-subspaces is possible. We measure the appearance of the 2 of $(D_{ISA}/2)$ -dimensional blocks for the *Beatles* songs by means of the Amari-index. The results, which demonstrate the success of our method, are shown in Figure 7. It can be seen that the JFD method found the hidden components, for 50 and 75 thousand samples for $L = 30$ (convolution length is 31) too. The number of sweeps required for the optimization of the permutations was between 1 and 6 for all sample numbers $1,000 \leq T \leq 75,000$, parameters $1 \leq L \leq 30$ and for all 50 random initializations. According to Table 5, for sample number $T = 75,000$ the Amari-index is between 1.07% ($L = 1$) and 4.43% ($L = 30$) on the average and has a small (0.04 – 0.09) standard deviation. Separation of the 2 of $D_{ISA}/2$ dimensional subspaces are illustrated in Figure 8 through the Hinton-diagrams.

$L = 1$	$L = 2$	$L = 5$	$L = 10$	$L = 20$	$L = 30$
1.07% (± 0.04)	1.43% (± 0.09)	2.29% (± 0.07)	3.31% (± 0.06)	4.03% (± 0.06)	4.43% (± 0.04)

Table 5: Amari-index of the JFD method for *Beatles* database for different convolution lengths: average \pm deviation. Number of samples: $T = 75,000$. For other sample numbers between $1,000 \leq T < 75,000$ see Figure 7(a).

	$M = 2$	$M = 5$	$M = 10$	$M = 15$
KCCA	1.33% (± 0.48)	1.20% (± 0.17)	2.76% (± 2.86)	3.00% (± 2.21)
KGV	1.26% (± 0.54)	1.18% (± 0.17)	1.51% (± 0.31)	1.54% (± 0.34)

Table 6: Amari-index for the KCCA and the KGV methods for database *ABC*, for different component number M : average \pm deviation. Number of samples: $T = 5,000$. For other sample numbers between $100 \leq T < 5,000$, see Figure 9.

5.3.2 Kernel-ISA Techniques

We study the efficiency of the KCCA and KGV kernel-ISA methods of Section 4.1.2. The kernel-ISA techniques was found to have a higher computational burden, but they also have advantages compared with the JFD technique for ISA tasks.

For the KCCA and KGV methods we also applied the pseudocode of Table 2. ICA was executed by the fastICA algorithm [56]. The Gaussian kernel $k(\mathbf{u}, \mathbf{v}) \propto \exp\left(\frac{-\|\mathbf{u}-\mathbf{v}\|^2}{2\sigma^2}\right)$ was chosen for both the KCCA and KGV methods and parameter σ was set to 5. In the KCCA method, regularization parameter $\kappa = 10^{-4}$ was applied. In the experiments, parameters (σ, κ) were proved to be reasonably robust. Mixing matrix \mathbf{A} was generated randomly from the orthogonal group and the sample number was chosen from the interval $100 \leq T \leq 5,000$.

Our first ISA example concerns the *ABC* database. The dimension of a component was $d = 2$ and the number of the components M took different values ($M = 2, 5, 10, 15$). Precision of the estimations is shown in Figure 9, where the precision of the JFD method on the same database is also depicted. The number of sweeps required for the optimization of the permutations is shown in Figure 10 for different sample numbers and for different component numbers. The data are averaged over 50 random estimations. Figure 11 depicts the KCCA estimation for the *ABC* database.

Figure 9 shows that the KCCA and KGV kernel-ISA methods give rise to high precision estimations on the *ABC* database even for small sample numbers. The KGV method was more precise for all M values studied than the JFD method. The ratio of precisions could be as high as 4 (see sample number 500). The KCCA method is somewhat weaker. For smaller tasks ($M = 2$ and 5) and for small sample numbers it also exceeds the precision of the JFD method. Precision of the method become about the same for higher sample numbers and larger tasks. Sweep numbers of the KCCA (KGV) method were between 2 and 8 (2 and 6) (Figure 10). Note that one sweep is always necessary for our procedure (Table 2). A single sweep may be satisfactory if—by chance—the ICA provides the correct permutation.

The other illustration concerns the *all-k-independent* database. This test can be difficult for ISA methods [35]. Number of components M was 2. For $k = 2, 3$, when the dimension of the components $d = 3$ and 4, respectively, the KCCA and KGV kernel-ISA methods efficiently estimated the hidden components. The precision of the KCCA and KGV estimations as well as the comparison with the JFD method are shown in Figure 12. The average number of sweeps required for the optimization of the permutations for different k values and for 50 randomly initialized computations is provided in Figure 13. The values of the Amari-indices are shown in Table 7.

According to Figure 12 the two kernel-based methods exhibit similar precision. Both were superior to the

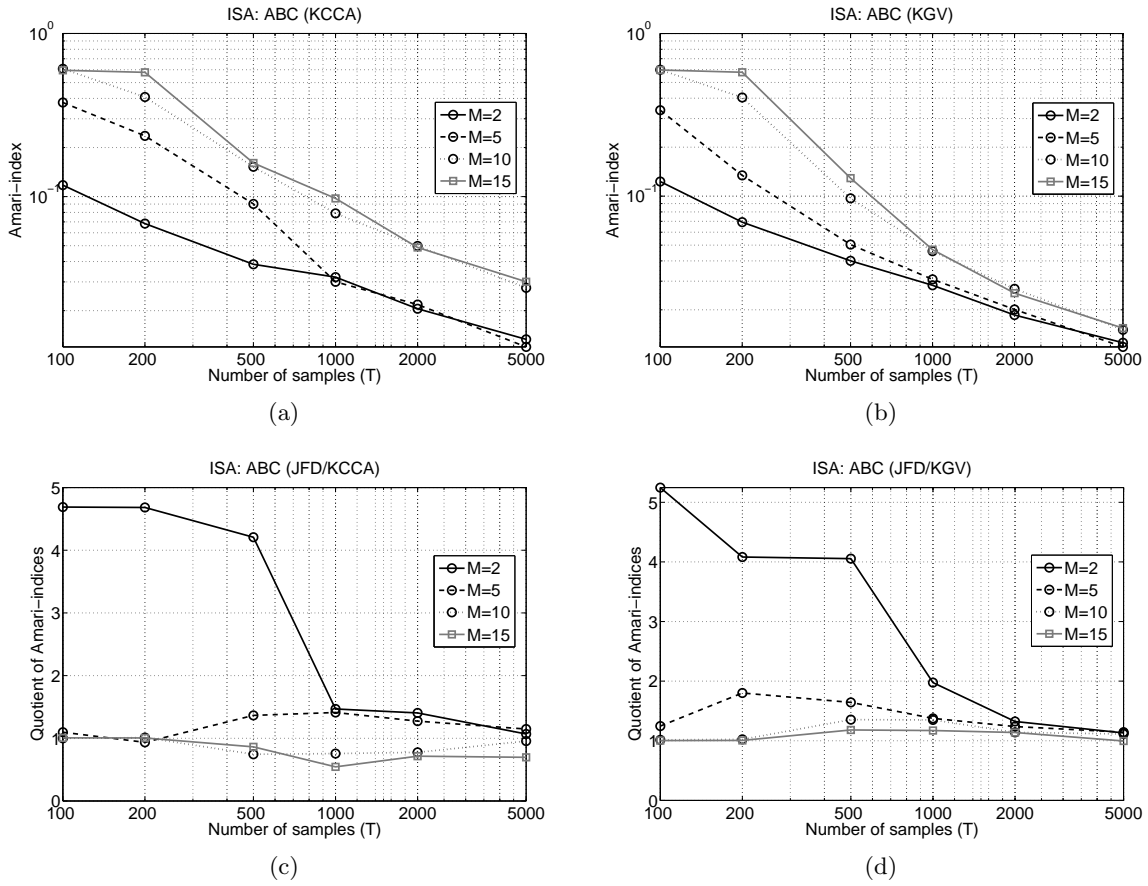


Figure 9: (a) and (b): Amari-index of the KCCA and KGV methods, respectively, for the *ABC* database as a function of sample number and for different numbers of components M . (c) and (d): Amari-index of the JFD method is divided by the Amari-index of the KCCA method and the KGV technique, respectively. For values larger (smaller) than 1 the kernel-ISA method is better (worse) than the JFD method.

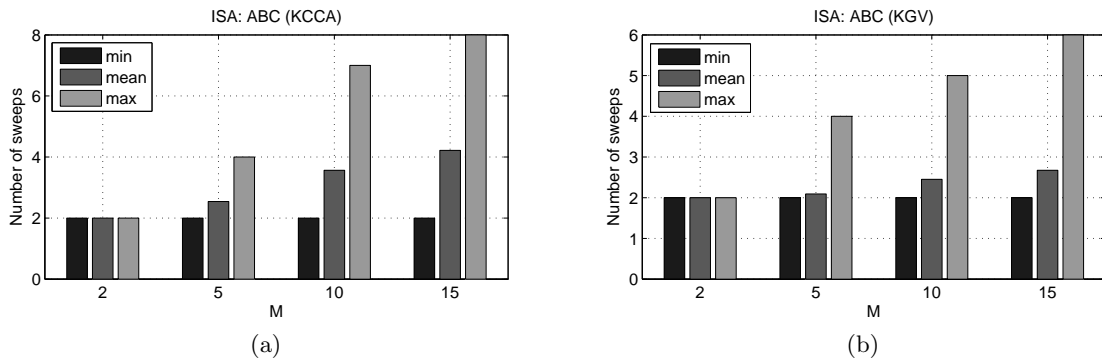


Figure 10: Number of sweeps for the KCCA and the KGV methods needed for the optimization of permutations as a function of component number M on the *ABC* database. (a): KCCA method, (b): KGV method. Black: minimum, gray: mean, light gray: maximum.

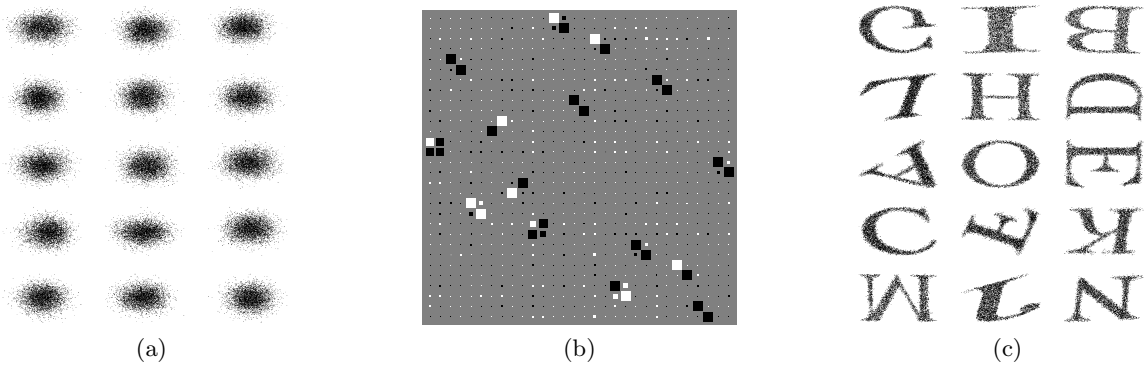


Figure 11: Illustration of the KCCA method for the *ABC* database. Sample number: $T = 5,000$. (a): observed mixed signals $\mathbf{x}(t)$. (b) Hinton-diagram: the product of the mixing matrix of the derived ISA task and the estimated demixing matrix (= approximately block-permutation matrix). (c): estimated components. Hidden components are recovered up to permutation and orthogonal transformation.

	$k = 2$	$k = 3$
KCCA/KGV	0.0017% (± 0.0014)	0.16% (± 0.04)

Table 7: The Amari-index of the KCCA and KGV methods for database *all-k-independent* for different k values: average \pm deviation. Number of samples: $T = 5,000$. For other sample numbers between $100 \leq T < 5,000$, see Figure 12.

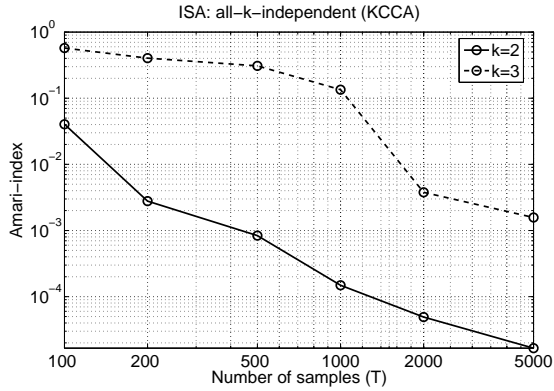
JFD technique. The ratio of the Amari-indices for sample number 5,000 and for $k = 2$ is more than 15,000, for $k = 3$ it is more than 500. For details concerning the Amari-indices, see Table 7. These indices are close to each other for the KCCA and the KGV methods: 0.0017% for $k = 2$, 0.16% for $k = 3$ on average. Both kernel-ISA methods used 2 – 3 sweeps for the optimization of the permutations (Figure 13).

6 Conclusions

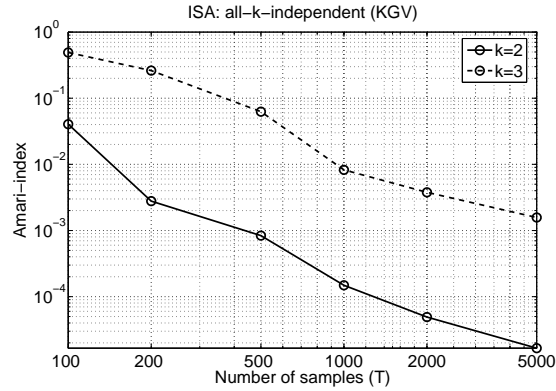
We have introduced a new model, the blind subspace deconvolution (BSSD) for data analysis. This model deals with the casual convolutive mixture of multidimensional independent sources. The undercomplete version (uBSSD) of the task has been presented, and it has been shown how to derive an independent subspace analysis (ISA) task from the uBSSD problem. Recent developments of the ISA techniques enabled us to handle the emerging high dimensional problems. Our earlier results, namely the ISA Separation Theorem [34] motivated us to reduce the ISA task to the search for the optimal permutation of the ICA components. The components were grouped with a novel joint decorrelation technique, the joint f-decorrelation (JFD) method [17].

Also, we adapted other ICA techniques, such as the KCCA and KGV methods to the ISA task and studied their efficiency. Simulations indicated that although the KCCA and KGV methods give rise to serious computational burden relative to the JFD method, they can be advantageous for smaller ISA tasks and for ISA tasks when the number of samples is small.

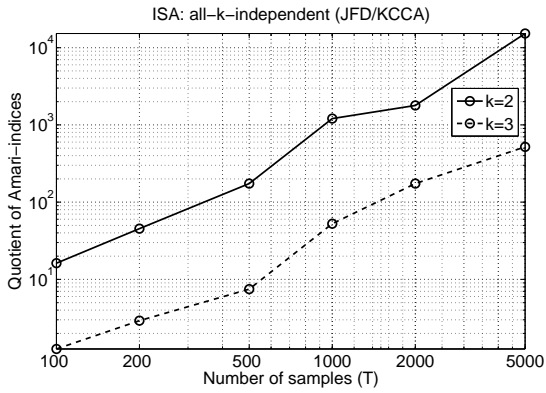
Finally, we note that we achieved small errors in these high dimensional computations. These small errors indicate that the Separation Theorem is robust and might be extended to a larger class of noise sources.



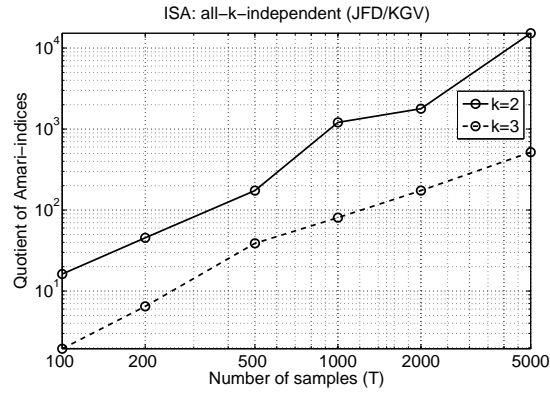
(a)



(b)

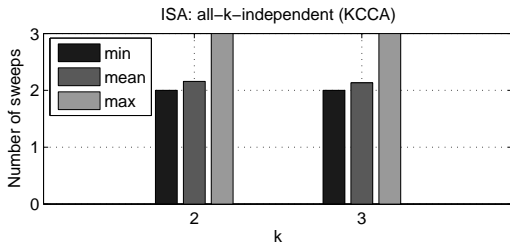


(c)

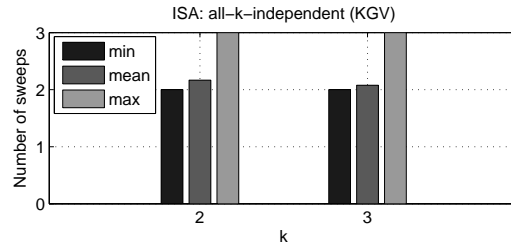


(d)

Figure 12: (a) and (b): Amari-indices of the KCCA and KGV methods, respectively, as a function of the sample number and for $k = 2$ and 3 on the *all-k-independent* database. For more details, see Table 7. (c): ratio of Amari-indices of JFD and KCCA methods, (d): ratio of Amari-indices of JFD and KGV methods.



(a)



(b)

Figure 13: Number of sweeps of permutation optimization for the KCCA (a) and KGV (b) methods for the *all-k-independent* database and for different k values. Black: minimum, gray: mean, light gray: maximum.

A Proof of the ISA Separation Theorem

We shall rely on entropy inequalities (Section A.1). In Section A.2 connection to the ICA cost function is derived (Lemma 2). The ISA Separation Theorem then follows.

A.1 EPI-type Relations

First, consider the so-called entropy power inequality (EPI)

$$e^{2H(\sum_{i=1}^L u_i)} \geq \sum_{i=1}^L e^{2H(u_i)},$$

where $u_1, \dots, u_L \in \mathbb{R}$ denote continuous random variables. This inequality holds, for example, for independent continuous variables [39].

If EPI is satisfied on the surface of the L -dimensional unit sphere \mathcal{S}^L , then a further inequality holds:

Lemma 1 *Suppose that continuous random variables $u_1, \dots, u_L \in \mathbb{R}$ satisfy the following inequality*

$$e^{2H(\sum_{i=1}^L w_i u_i)} \geq \sum_{i=1}^L e^{2H(w_i u_i)}, \forall \mathbf{w} \in \mathcal{S}^L. \quad (16)$$

This inequality will be called the w-EPI condition. Then Equation (8) holds, too.

Proof *Assume that $\mathbf{w} \in \mathcal{S}^L$. Applying \ln on condition (16), and using the monotonicity of the \ln function, we can see that the first inequality is valid in the following inequality chain*

$$\begin{aligned} 2H\left(\sum_{i=1}^L w_i u_i\right) &\geq \ln\left(\sum_{i=1}^L e^{2H(w_i u_i)}\right) = \ln\left(\sum_{i=1}^L e^{2H(u_i)} w_i^2\right) \\ &\geq \sum_{i=1}^L w_i^2 \ln\left(e^{2H(u_i)}\right) = 2 \sum_{i=1}^L w_i^2 H(u_i). \end{aligned}$$

Here,

1. we used the relation

$$H(w_i u_i) = H(u_i) + \ln(|w_i|)$$

for the entropy of the transformed variable [39]. Hence

$$e^{2H(w_i u_i)} = e^{2H(u_i) + 2\ln(|w_i|)} = e^{2H(u_i)} e^{2\ln(|w_i|)} = e^{2H(u_i)} w_i^2.$$

2. In the second inequality, the concavity of \ln was exploited. \square

Note 5 *w-EPI holds, for example, for independent variables u_i , because independence is not affected by multiplication with a constant.*

A.2 Connection to the Cost Function of the ICA Task

The ISA Separation Theorem will be a corollary of the following claim:

Lemma 2 Let $\mathbf{y} = [\mathbf{y}^1; \dots; \mathbf{y}^M] = \mathbf{y}(\mathbf{W}) = \mathbf{W}\mathbf{s} \in \mathbb{R}^D$, where $\mathbf{W} \in \mathcal{O}^D$ ($D = \sum_{m=1}^M d_m$), $\mathbf{y}^m \in \mathbb{R}^{d_m}$ is the estimation of the m^{th} component of the ISA task. Let $y_i^m \in \mathbb{R}$ be the i^{th} coordinate of the m^{th} component ($i = 1, \dots, d_m$). Similarly, let $s_i^m \in \mathbb{R}$ stand for the i^{th} coordinate of the m^{th} source. Let us assume that the $\mathbf{u} := \mathbf{s}^m \in \mathbb{R}^{d_m}$ sources satisfy the condition (8). Then

$$\sum_{m=1}^M \sum_{i=1}^{d_m} H(y_i^m) \geq \sum_{m=1}^M \sum_{i=1}^{d_m} H(s_i^m). \quad (17)$$

Proof Let us denote the $(i, j)^{\text{th}}$ element of matrix \mathbf{W} by $W_{i,j}$. Coordinates of \mathbf{y} and \mathbf{s} will be denoted by y_i and s_i , respectively. Further, let \mathcal{G}^m denote the indices of the m^{th} subspace ($m = 1, \dots, M$), that is, $\mathcal{G}^m := \{1 + \sum_{i=1}^{m-1} d_i, \dots, \sum_{i=1}^m d_i\}$ ($d_0 := 0$). Now, writing the elements of the i^{th} row of matrix multiplication $\mathbf{y} = \mathbf{W}\mathbf{s}$, we have

$$y_i = \sum_{j \in \mathcal{G}^1} W_{i,j} s_j + \dots + \sum_{j \in \mathcal{G}^M} W_{i,j} s_j \quad (18)$$

and thus,

$$H(y_i) = H\left(\sum_{m=1}^M \sum_{j \in \mathcal{G}^m} W_{i,j} s_j\right) \quad (19)$$

$$= H\left(\sum_{m=1}^M \left[\left(\sum_{l \in \mathcal{G}^m} W_{i,l}^2\right)^{\frac{1}{2}} \frac{\sum_{j \in \mathcal{G}^m} W_{i,j} s_j}{\left(\sum_{l \in \mathcal{G}^m} W_{i,l}^2\right)^{\frac{1}{2}}} \right]\right) \quad (20)$$

$$\geq \sum_{m=1}^M \left[\left(\sum_{l \in \mathcal{G}^m} W_{i,l}^2\right) H\left(\frac{\sum_{j \in \mathcal{G}^m} W_{i,j} s_j}{\left(\sum_{l \in \mathcal{G}^m} W_{i,l}^2\right)^{\frac{1}{2}}}\right) \right] \quad (21)$$

$$= \sum_{m=1}^M \left[\left(\sum_{l \in \mathcal{G}^m} W_{i,l}^2\right) H\left(\sum_{j \in \mathcal{G}^m} \frac{W_{i,j}}{\left(\sum_{l \in \mathcal{G}^m} W_{i,l}^2\right)^{\frac{1}{2}}} s_j\right) \right] \quad (22)$$

$$\geq \sum_{m=1}^M \left[\left(\sum_{l \in \mathcal{G}^m} W_{i,l}^2\right) \sum_{j \in \mathcal{G}^m} \left(\frac{W_{i,j}}{\left(\sum_{l \in \mathcal{G}^m} W_{i,l}^2\right)^{\frac{1}{2}}}\right)^2 H(s_j) \right] \quad (23)$$

$$= \sum_{j \in \mathcal{G}^1} W_{i,j}^2 H(s_j) + \dots + \sum_{j \in \mathcal{G}^M} W_{i,j}^2 H(s_j). \quad (24)$$

The above steps can be justified as follows:

1. (19): Equation (18) was inserted into the argument of H .
2. (20): New terms were added for Lemma 1.
3. (21): Sources \mathbf{s}^m are independent of one another and this independence is preserved upon mixing within the subspaces, and we could also use Lemma 1, because \mathbf{W} is an orthogonal matrix.

4. (22): Nominators were transferred into the \sum_j terms.
5. (23): Variables \mathbf{s}^m satisfy condition (8) according to our assumptions.
6. (24): We simplified the expression after squaring.

Using this inequality, summing it for i , exchanging the order of the sums, and making use of the orthogonality of matrix \mathbf{W} , we have

$$\begin{aligned}
\sum_{i=1}^D H(y_i) &\geq \sum_{i=1}^D \left(\sum_{j \in \mathcal{G}^1} W_{i,j}^2 H(s_j) + \dots + \sum_{j \in \mathcal{G}^M} W_{i,j}^2 H(s_j) \right) \\
&= \sum_{j \in \mathcal{G}^1} \left(\sum_{i=1}^D W_{i,j}^2 \right) H(s_j) + \dots + \sum_{j \in \mathcal{G}^M} \left(\sum_{i=1}^D W_{i,j}^2 \right) H(s_j) \\
&= \sum_{j=1}^D H(s_j). \quad \square
\end{aligned}$$

Corollary (ISA Separation Theorem) ICA minimizes the l.h.s. of Equation (17), that is, it minimizes $\sum_{m=1}^M \sum_{i=1}^{d_m} H(y_i^m)$. The set of minima is invariant to permutations and to changes of the signs. Also, according to Proposition 2, $\{\mathbf{s}_i^m\}$, that is, the coordinates of the \mathbf{s}^m components of the ISA task belong to the set of the minima. \square

B Kernel Covariance Technique for the ISA Task

For the sake of completeness, the extension of the KC method [48] for the ISA task is detailed below. The extension is similar to the extensions presented in Section 4.1.2 (see the KCCA method), and we use the notations of that section.

First, we would like to measure the dependence of two 2 random variables $\mathbf{u} \in \mathbb{R}^{d_1}$ and $\mathbf{v} \in \mathbb{R}^{d_2}$. The KC technique defines their dependence as their maximal covariance on the unit spheres $\mathcal{S}^{\mathbf{u}}$, $\mathcal{S}^{\mathbf{v}}$ of function spaces $\mathcal{F}^{\mathbf{u}}$, $\mathcal{F}^{\mathbf{v}}$:

$$J_{\text{KC}}(\mathbf{u}, \mathbf{v}, \mathcal{F}^{\mathbf{u}}, \mathcal{F}^{\mathbf{v}}) := \sup_{g \in \mathcal{S}^{\mathbf{u}}, h \in \mathcal{S}^{\mathbf{v}}} |E\{[g(\mathbf{u}) - Eg(\mathbf{u})][h(\mathbf{v}) - Eh(\mathbf{v})]\}|.$$

This function J_{KC} can be estimated empirically from T -element samples $\mathbf{u}_1, \dots, \mathbf{u}_T \in \mathbb{R}^{d_1}$, $\mathbf{v}_1, \dots, \mathbf{v}_T \in \mathbb{R}^{d_2}$:

$$J_{\text{KC}}^{\text{emp}}(\mathbf{u}, \mathbf{v}, \mathcal{F}^{\mathbf{u}}, \mathcal{F}^{\mathbf{v}}) := \sup_{g \in \mathcal{S}^{\mathbf{u}}, h \in \mathcal{S}^{\mathbf{v}}} \left| \frac{1}{T} \sum_{t=1}^T [g(\mathbf{u}_t) - \bar{g}][h(\mathbf{v}_t) - \bar{h}] \right|.$$

The estimation can be reduced to the following conditional maximization problem:

$$J_{\text{KC}}^{\text{emp}}(\mathbf{u}, \mathbf{v}, \mathcal{F}^{\mathbf{u}}, \mathcal{F}^{\mathbf{v}}) = \sup_{\mathbf{c}_1^* \tilde{\mathbf{K}}^{\mathbf{u}} \mathbf{c}_1 \leq 1, \mathbf{c}_2^* \tilde{\mathbf{K}}^{\mathbf{v}} \mathbf{c}_2 \leq 1} \mathbf{c}_1^* \tilde{\mathbf{K}}^{\mathbf{u}} \tilde{\mathbf{K}}^{\mathbf{v}} \mathbf{c}_2. \quad (25)$$

After the adaptation of the Lagrange multiplier technique and the computation of the stationary points of (25) it can be realized that the values of $[\mathbf{c}_1; \mathbf{c}_2]$ and $J_{\text{KC}}^{\text{emp}}$ can be computed as the solutions of the generalized eigenvalue problem

$$\begin{pmatrix} \tilde{\mathbf{K}}^{\mathbf{u}} & \tilde{\mathbf{K}}^{\mathbf{u}} \tilde{\mathbf{K}}^{\mathbf{v}} \\ \tilde{\mathbf{K}}^{\mathbf{v}} \tilde{\mathbf{K}}^{\mathbf{u}} & \tilde{\mathbf{K}}^{\mathbf{v}} \end{pmatrix} \begin{pmatrix} \mathbf{c}_1 \\ \mathbf{c}_2 \end{pmatrix} = \lambda \begin{pmatrix} \tilde{\mathbf{K}}^{\mathbf{u}} & \mathbf{0} \\ \mathbf{0} & \tilde{\mathbf{K}}^{\mathbf{v}} \end{pmatrix} \begin{pmatrix} \mathbf{c}_1 \\ \mathbf{c}_2 \end{pmatrix}. \quad (26)$$

If the task is to measure the dependence between more than two random variables $\mathbf{y}^1 \in \mathbb{R}^{d_1}, \dots, \mathbf{y}^M \in \mathbb{R}^{d_M}$ then (26) is to be replaced with the following generalized eigenvalue problem:

$$\begin{pmatrix} \tilde{\mathbf{K}}^1 & \tilde{\mathbf{K}}^1 \tilde{\mathbf{K}}^2 & \dots & \tilde{\mathbf{K}}^1 \tilde{\mathbf{K}}^M \\ \tilde{\mathbf{K}}^2 \tilde{\mathbf{K}}^1 & \tilde{\mathbf{K}}^2 & \dots & \tilde{\mathbf{K}}^2 \tilde{\mathbf{K}}^M \\ \vdots & \vdots & \ddots & \vdots \\ \tilde{\mathbf{K}}^M \tilde{\mathbf{K}}^1 & \tilde{\mathbf{K}}^M \tilde{\mathbf{K}}^2 & \dots & \tilde{\mathbf{K}}^M \end{pmatrix} \begin{pmatrix} \mathbf{c}_1 \\ \mathbf{c}_2 \\ \vdots \\ \mathbf{c}_M \end{pmatrix} = \lambda \begin{pmatrix} \tilde{\mathbf{K}}^1 & \mathbf{0} & \dots & \mathbf{0} \\ \mathbf{0} & \tilde{\mathbf{K}}^2 & \dots & \mathbf{0} \\ \vdots & \vdots & \ddots & \vdots \\ \mathbf{0} & \mathbf{0} & \dots & \tilde{\mathbf{K}}^M \end{pmatrix} \begin{pmatrix} \mathbf{c}_1 \\ \mathbf{c}_2 \\ \vdots \\ \mathbf{c}_M \end{pmatrix}.$$

Using the maximal eigenvalue of this problem, J_{KC} can be estimated.

References

- [1] Jutten, C., Herault, J.: Blind separation of sources: An adaptive algorithm based on neuromimetic architecture. *Signal Processing* **24** (1991) 1–10
- [2] Comon, P.: Independent component analysis, a new concept? *Signal Processing* **36** (1994) 287–314
- [3] Hyvärinen, A., Karhunen, J., Oja, E.: *Independent Component Analysis*. John Wiley & Sons (2001)
- [4] Cichocki, A., Amari, S.: *Adaptive Blind Signal and Image Processing*. John Wiley & Sons (2002)
- [5] Hyvärinen, A., Hoyer, P.O.: Emergence of phase and shift invariant features by decomposition of natural images into independent feature subspaces. *Neural Computation* **12** (2000) 1705–1720
- [6] Cardoso, J.: Multidimensional independent component analysis. In: *Proceedings of International Conference on Acoustics, Speech, and Signal Processing (ICASSP '98)*. Volume 4., Seattle, WA, USA (1998) 1941–1944
- [7] Theis, F.J.: Blind signal separation into groups of dependent signals using joint block diagonalization. In: *Proceedings of International Society for Computer Aided Surgery (ISCAS 2005)*, Kobe, Japan (2005) 5878–5881
- [8] Akaho, S., Kiuchi, Y., Umeyama, S.: MICA: Multimodal independent component analysis. In: *Proceedings of International Joint Conference on Neural Networks (IJCNN '99)*. (1999) 927–932
- [9] Hyvärinen, A., Köster, U.: FastISA: A fast fixed-point algorithm for independent subspace analysis. In: *Proceedings of European Symposium on Artificial Neural Networks (ESANN 2006)*, Bruges, Belgium (2006)
- [10] Vollgraf, R., Obermayer, K.: Multi-dimensional ICA to separate correlated sources. In: *Proceedings of Neural Information Processing Systems (NIPS 2001)*. Volume 14. (2001) 993–1000
- [11] Bach, F.R., Jordan, M.I.: Beyond independent components: Trees and clusters. *Journal of Machine Learning Research* **4** (2003) 1205–1233
- [12] Stögbauer, H., Kraskov, A., Astakhov, S.A., Grassberger, P.: Least dependent component analysis based on mutual information. *Physical Review E - Statistical, Nonlinear, and Soft Matter Physics* **70** (2004)
- [13] Póczos, B., Lőrincz, A.: Independent subspace analysis using k-nearest neighborhood distances. *Artificial Neural Networks: Formal Models and their Applications - ICANN 2005, pt 2, Proceedings* **3697** (2005) 163–168

- [14] Póczos, B., Lőrincz, A.: Independent subspace analysis using geodesic spanning trees. In: Proceedings of International Conference on Machine Learning (ICML 2005), Bonn, Germany (2005) 673–680
- [15] Theis, F.J.: Multidimensional independent component analysis using characteristic functions. In: Proceedings of European Signal Processing Conference (EUSIPCO 2005). (2005)
- [16] Theis, F.J.: Towards a general independent subspace analysis. In: Proceedings of Neural Information Processing Systems (NIPS 2006). (2006)
- [17] Szabó, Z., Lőrincz, A.: Real and complex independent subspace analysis by generalized variance. In: Proceedings of ICA Research Network International Workshop (ICARN 2006), Liverpool, U.K. (2006) 85–88 <http://arxiv.org/abs/math.ST/0610438>.
- [18] Nolte, G., Meinecke, F.C., Ziehe, A., Müller, K.R.: Identifying interactions in mixed and noisy complex systems. *Physical Review E* **73** (2006)
- [19] Pedersen, M.S., Larsen, J., Kjems, U., Parra, L.C.: A survey of convolutive blind source separation methods. In: Springer Handbook of Speech (to appear). Springer Press (2007)
- [20] MacDonald, A., Cain, S.: Derivation and application of an anisoplanatic optical transfer function for blind deconvolution of laser radar imagery. *Unconventional Imaging* **5896** (2005) 9–20
- [21] Hedgepeth, J.B., Gallucci, V.F., O’Sullivan, F., Thorne, R.E.: An expectation maximization and smoothing approach for indirect acoustic estimation of fish size and density. *ICES Journal of Marine Science* **56** (1999) 36–50
- [22] Vural, C., Sethares, W.A.: Blind image deconvolution via dispersion minimization. *Digital Signal Processing* **16** (2006) 137–148
- [23] Douglas, S.C., Sawada, H., Makino, S.: Natural gradient multichannel blind deconvolution and speech separation using causal FIR filters. *IEEE Transactions on Speech and Audio Processing* **13** (2005) 92–104
- [24] Mitianoudis, N., Davies, M.E.: Audio source separation of convolutive mixtures. *IEEE Transactions on Speech and Audio Processing* **11** (2003) 489–497
- [25] Roan, M.J., Gramann, M.R., Erling, J.G., Sibul, L.H.: Blind deconvolution applied to acoustical systems identification with supporting experimental results. *The Journal of the Acoustical Society of America* **114** (2003) 1988–1996
- [26] Araki, S., Makino, S., Mukai, R., Nishikawa, T., Saruwatari, H.: Fundamental limitation of frequency domain blind source separation for convolved mixture of speech. *IEEE Transactions on Speech and Audio Processing* **11** (2003) 109–116
- [27] Akyildiz, I.F., Su, W., Sankarasubramaniam, Y., Cayirci, E.: Wireless sensor networks: a survey. *Computer Networks* **38** (2002) 393–422
- [28] Deligianni, F., Lo, B., Yang, G.: Source recovery for body sensor network. In: Proceedings of International Workshop on Wearable and Implantable Body Sensor Networks 2006 (BSN 2006). (2006) 199–202
- [29] Jung, T., Makeig, S., Lee, T., McKeown, M.J., Brown, G., Bell, A.J., Sejnowski, T.J.: Independent component analysis of biomedical signals. In: Proceedings of International Workshop on Independent Component Analysis and Signal Separation (ICA 2000), Helsinki (2000) 633–644

- [30] Glover, G.H.: Deconvolution of impulse response in event-related BOLD fMRI. *NeuroImage* **9** (1999) 416–429
- [31] Dyrholm, M., Makeig, S., Hansen, L.K.: Model selection for convolutive ICA with an application to spatio-temporal analysis of EEG. *Neural Computation* (2007)
- [32] Kotzer, T., Cohen, N., Shamir, J.: Generalized projection algorithms with applications to optics and signal restoration. *Optics Communications* **156** (1998) 77–91
- [33] Karshi, H.: Further improvement of temporal resolution of seismic data by autoregressive (AR) spectral extrapolation. *Journal of Applied Geophysics* **59** (2006) 324–336
- [34] Szabó, Z., Póczos, B., Lőrincz, A.: Separation theorem for \mathbb{K} -independent subspace analysis with sufficient conditions. Technical report, Eötvös Loránd University, Budapest (2006) <http://arxiv.org/abs/math.ST/0608100>.
- [35] Szabó, Z., Póczos, B., Lőrincz, A.: Cross-entropy optimization for independent process analysis. In: *Proceedings of Independent Component Analysis and Blind Signal Separation (ICA 2006)*. Volume 3889 of LNCS., Springer (2006) 909–916
- [36] Bach, F.R., Jordan, M.I.: Kernel independent component analysis. *Journal of Machine Learning Research* **3** (2002) 1–48
- [37] Rajagopal, R., Potter, L.C.: Multivariate MIMO FIR inverses. *IEEE Transactions on Image Processing* **12** (2003) 458 – 465
- [38] Theis, F.J.: Uniqueness of complex and multidimensional independent component analysis. *Signal Processing* **84** (2004) 951–956
- [39] Cover, T.M., Thomas, J.A.: *Elements of Information Theory*. John Wiley and Sons, New York, USA (1991)
- [40] Févotte, C., Doncarli, C.: A unified presentation of blind source separation for convolutive mixtures using block-diagonalization. In: *Proceedings of Independent Component Analysis and Blind Signal Separation (ICA 2003)*, Nara, Japan (2003) 349–354
- [41] Abed-Meraim, K., Belouchrani, A.: Algorithms for joint block diagonalization. In: *Proceedings of European Signal Processing Conference (EUSIPCO 2004)*. (2004) 209–212
- [42] Fang, K.T., Kotz, S., Ng, K.W.: *Symmetric Multivariate and Related Distributions*. Chapman and Hall (1990)
- [43] Takano, S.: The inequalities of Fisher information and entropy power for dependent variables. In: *Symposium on Probability Theory and Mathematical Statistics*. (1995)
- [44] Aronszajn, N.: Theory of reproducing kernels. *Transactions of the American Mathematical Society* **68** (1950) 337–404
- [45] Wahba, G.: Support vector machines, reproducing kernel hilbert spaces, and randomized GACV. In: *Advances in Kernel Methods*, MIT Press (1999) 69–88
- [46] Schölkopf, B., Burges, C.J.C., Smola, A.J.: *Advances in Kernel Methods - Support Vector Learning*. MIT Press, Cambridge, MA (1999)

- [47] Fukumizu, K., Bach, F.R., Gretton, A.: Statistical consistency of kernel canonical correlation analysis. *Journal of Machine Learning Research* **8** (2007) 361–383
- [48] Gretton, A., Smola, A., Bousquet, O., Schölkopf, B.: Kernel methods for measuring independence. *Journal of Machine Learning Research* **6** (2005) 2075–2129
- [49] Edelman, A., Arias, T., Smith, S.T.: The geometry of algorithms with orthogonality constraints. *SIAM Journal on Matrix Analysis and Applications* **20** (1998) 303–353
- [50] Lippert, R.A.: Nonlinear Eigenvalue Problems. PhD thesis, Massachusetts Institute of Technology (1998)
- [51] Plumbley, M.D.: Lie group methods for optimization with orthogonality constraints. In: *Proceedings of Independent Component Analysis and Blind Signal Separation (ICA 2004)*. Volume 3195 of LNCS., Springer (2004) 1245–1252
- [52] Quinquis, N., Yamada, I., Sakaniwa, K.: Efficient dual Cayley parametrization technique for ICA with orthogonality constraints. In: *Proceedings of ICA Research Network International Workshop (ICARN 2006)*, Liverpool, U.K. (2006) 123–126
- [53] Nishimori, Y., Akaho, S., Plumbley, M.D.: Riemannian optimization method on the flag manifold for independent subspace analysis. In: *Proceedings of Independent Component Analysis and Blind Signal Separation (ICA 2006)*. Volume 3889 of LNCS., Springer (2006) 295–302
- [54] Póczos, B., Lórinicz, A.: Non-combinatorial estimation of independent autoregressive sources. *Neurocomputing Letters* **69** (2006) 2416–2419
- [55] Amari, S., Cichocki, A., Yang, H.H.: A new learning algorithm for blind signal separation. *Advances in Neural Information Processing Systems* **8** (1996) 757–763
- [56] Hyvärinen, A., Oja, E.: A fast fixed-point algorithm for independent component analysis. *Neural Computation* **9** (1997) 1483–1492